Die approbierte Originalversion dieser Diplom-/Masterarbeit ist an der Hauptbibliothek der Technischen Universität Wien aufgestellt (http://www.ub.tuwien.ac.at).

The approved original version of this diploma or master thesis is available at the main library of the Vienna University of Technology (http://www.ub.tuwien.ac.at/englweb/).

TECHNISCHE UNIVERSITÄT WIEN
Vienna University of Technology

DIPLOMARBEIT

SYNTHESIS AND CHARACTERIZATION OF NEW IRON CARBONYL AND HYDRIDE COMPLEXES

ausgeführt am Institut für

Angewandte Synthesechemie

der Technischen Universität Wien

unter der Anleitung von

Ao.Univ.Prof. DI Dr.techn. Karl Kirchner

und Projektass. DI Bernhard Bichler

durch

Marlene Möller

Staudgasse 44/6

1180 Wien

Wien, am 24. Mai 2012

Für meine Eltern:
Susanne und Harald

Abstract

The aim of this work was to investigate CO binding to different kinds of Fe(II) PNP pincer complexes and to synthesize a hydride species that can be used for catalysis of hydrogenation reactions. The second goal was to find new PNP pincer ligands that increase the solubility of the FePNP-complexes for better analysis and application.

In the first part of this thesis the synthesis of the ligand systems used is described. Several known tridentate ligands were synthesized and based on their synthetic routes new ligand systems could be obtained. These products were characterized by NMR spectroscopy.

In the second part of this work the CO binding to complexes formed from iron(II)chloride and the above mentioned pincer ligands was investigated. The complexes were analyzed by NMR and IR spectroscopy and X-ray crystallography. The binding of CO is important because it is assumed, that it is a crucial co-ligand for hydrogenation catalysts.

The last objective of this work was to synthesize hydride species of the FePNP complexes via various routes. It was tried to first reduce the Fe(II) precursor to a Fe(0) species and then do a oxidative addition of HX (X = Cl^-, BF_4^-,...), which resulted in the desired product but in very low yields. Reactions with Fe(II) precursors with superhydride ($LiEt_3BH$) gave only wild mixtures of products. When it was discovered that a hydride species is formed when the $[Fe(II)PNP(CO)_2Cl]^+$ precursors were reacted with Zn this route was further investigated but could not yield clean products until now.

Kurzfassung

Das Ziel dieser Arbeit war es das Additionsverhalten von CO an verschiedene Fe(II) PNP Pincer Komplexe zu untersuchen und weiters die für die Katalyse von Hydrierungsreaktionen wichtigen Hydridspezies herzustellen.

Außerdem sollten neue PNP Pincer Liganden gefunden werden, die die Löslichkeit der FePNP-Komplexe erhöhen, um bessere Analyse und Einsetzbarkeit zu gewährleisten.

Im ersten Teil dieser Arbeit wird die Synthese der verwendeten Ligandensysteme beschrieben. Es wurden verschiedene, bereits bekannte dreizähnige Liganden synthetisiert, auf Basis deren Synthesewege neue Liganden entwickelt werden konnten. Die Produkte wurden mit NMR Spektroskopie charakterisiert.

Im zweiten Teil wurde die Addition von CO an Komplexe, welche aus Eisen(II)chlorid und den oben genannten Liganden erhalten wurden, untersucht. Die Komplexe wurden mittels NMR und IR Spektroskopie und Einkristallröntgendiffraktion untersucht. Die Koordination von CO ist ein wichtiges Forschungsgebiet, da vermutet wird, dass der Carbonyl-Ligand ein entscheidender Co-Ligand bei Hydrierungsreaktionen ist.

Im letzten Teil der Arbeit wurde auf verschiedene Arten versucht Hydridkomplexe aus den FePNP-Systemen herzustellen. Zunächst wurde die Fe(II) Vorstufe reduziert um dann eine oxidative Addition von HX (X = Cl^-, BF_4^-,...) durchzuführen, was auch gelang, allerdings nur in sehr geringen Ausbeuten. Reaktionen der Fe(II) Vorstufen mit Superhydrid ($LiEt_3BH$) resultierte in Produktmischungen mit sehr vielen Nebenprodukten. Nachdem wir entdeckten, dass sich eine Hydridspezies bildet, wenn die $[Fe(II)PNP(CO)_2Cl]^+$ Vorstufen mit Zn umgesetzt wurden, wurden einige Versuche in diese Richtung gestartet, allerdings konnte bis zu diesem Zeitpunkt kein sauberes Produkt isoliert werden.

Acknowledgments

First I want to thank Prof. Karl Kirchner for giving me the opportunity to work in his group, for his advice and the kind supervision.

Thanks to Prof. Mereiter for X-ray crystallography measurements.

I would like to thank Bernhard Bichler for the good teamwork and his help whenever needed and my colleagues Christian, Eva and Özgür for the nice working atmosphere.

Thanks to all my friends that I could share my good times with and whom I could always talk to when no one else was there.

Special thanks to my parents, who made my studies possible and were always encouraging me and supporting me both financially and mentally. Also I want to thank my sister, my grandparents, the rest of the family and Elisabeth for always being there.

Last but not least I would like to thank my fiancé for encouraging me whenever needed and his constructive criticism. I'm sure it was not always easy especially when I was stressed out before exams or big events.

Contents

1. Introduction and Scope

Catalysis of hydrogenation reactions of unsaturated functional groups is one of the most important topics in organic synthetic chemistry. Even more desirable are catalysts that yield enantiomerically pure products.

There is already a large amount of well-defined reduction catalysts known, but mostly transition-metals like ruthenium, rhodium, iridium, platinum or palladium are used. The catalysts containing these elements are highly active and selective, but are also expensive and toxic, which makes their use problematic for industrial purposes.

Therefore the research in this field is still ongoing and it is tried to find new well-defined highly active catalysts containing cheaper metals like copper, nickel, iron, manganese and zinc. The most obvious choice is iron due to the fact, that it is the most abundant transition-metal in the Earth's crust.

Already three examples for iron catalysts in the field of hydrogenation reactions have been reported in literature. Figure 1.2 shows the three of them, where **a** was described by Casey and Guan [1], **b** by Morris et al. [2] and **c** was described by Milstein and co-workers [3].

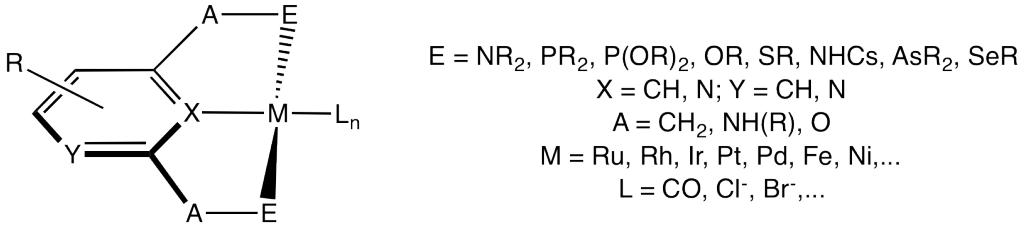

Figure 1.1: General structure of pincer complexes

In the last couple of years our research group is trying to develop catalysts featuring modular build bi- and tridentate ligands with aminophospine groups (Figure 1.1). The desired complexes all bear CO as co-ligand, as do all three examples mentioned above.

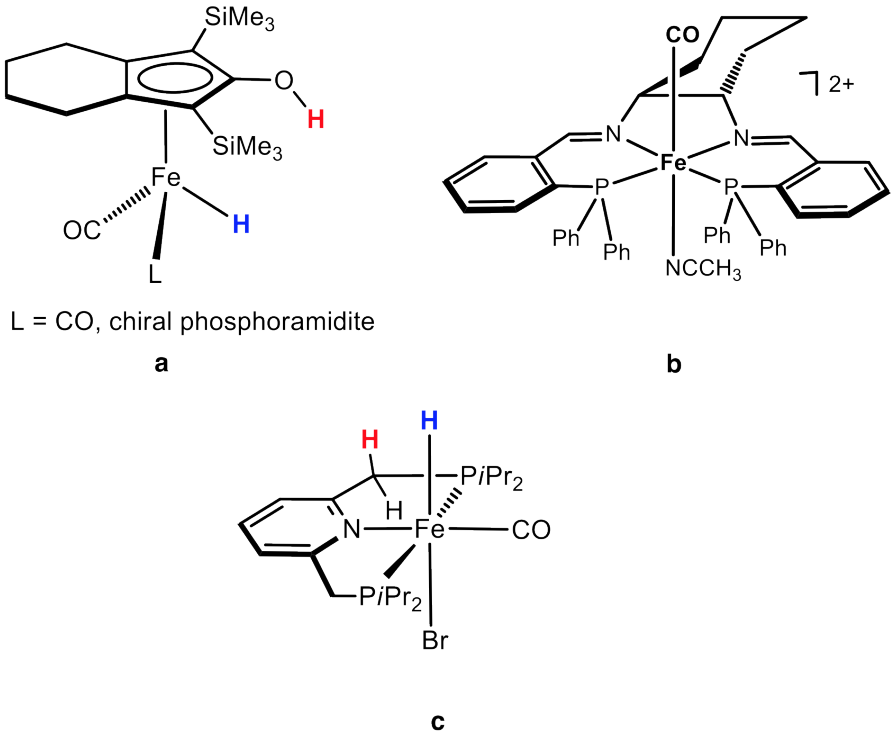

Figure 1.2: Well-defined iron complexes for hydrogenation reactions

It has also been reported that an Fe-CO moiety is present in the active site of hydrogenases [4], therefore it is reasonable to assume that carbonyl ligands are of vital importance for the activity of the catalyst.

The objective of this work was to investigate CO binding to different kinds of Fe(II) PNP pincer complexes and to try to synthesize the hydride species that can be used for catalysis. The second goal was to find new PNP pincer ligands that increase the solubility of the FePNP-complexes for better analysis and application.

Part I

GENERAL PART

2. PNP Ligands

The content of this chapter refers to the work published by Benito-Garagorri and Kirchner in 2008 [5].

Pincer ligands are neutral or anionic tridentate ligands with a central aromatic ring, that is *ortho*,*ortho*-disubstituted with two electron-donor substituents. Examples are shown in figure 2.1. There have also been reports of anionic pincer ligands without a aromatic ring in their backbone [6–9].

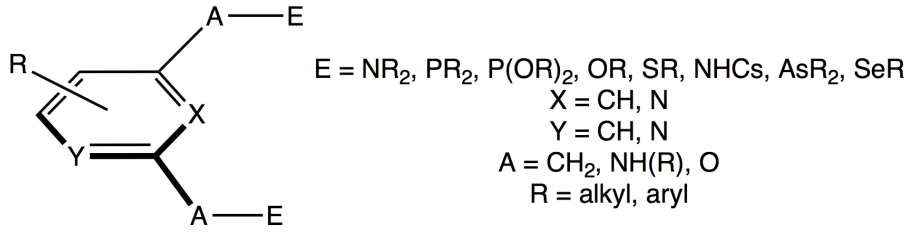

Figure 2.1: Different pincer ligands

The aromatic ring can be either a pyridine or pyrimidine or benzene ring. The substituents are connected to it via spacers, which can be methylene groups (-CH_2-), amines (-NR-) or oxygen atoms (-O-). Typically amines (NR_2), phosphines (PR_2), phosphites ($P(OR)_2$), ethers (OR) and thioethers (SR) are used as electron-donor substituents, but N-heterocyclic carbenes (NHCs), arsines (AsR_2) and selenoethers (SeR) are also suitable. However in most cases phosphines or phosphites are used. Pincer ligands with two different donor groups have also been reported [10–14].

Pincer ligands are easily variable and have high stability and activity, three properties that are very important in organometallic chemistry. They coordinate to the metal center via the two electron-donor groups and metal-nitrogen (for pyridine- or pyrimidine-based PNP pincer) or metal-carbon (for benzene-based PCP ligands) σ bonds.

They can be modified by variation of the aromatic ring used and its substitution, the donor groups and the spacers or combinations of the three.

The first pincer compounds have been reported in the 1970s [15–19], but they have not been much explored until the 1990s, when some applications were discovered. In catalysis for example they were used for C-C bond forming reactions, to investigate C-C, C-H and C-O bond activation, polymerization reactions, transfer hydrogenation and dehydrogenation reactions. Pincer complexes were also used as sensors and were serving as building blocks for self-assembled supramolecular structures [20, 21].

When amines are used as spacer groups an easy method to introduce different phosphines with one synthetic strategy using electrophilic chlorophosphines opens up. Both achiral and chiral phosphines can be introduced into the system this way. Already some applications in catalysis have been found for PNP complexes with aminophosphine groups: palladium PNP and PCP complexes are usable for Suzuki-Miyaura coupling reactions, iron PNP compounds for the coupling of aromatic aldehydes with ethyl diazoacetate to give 3-hydroxyacrylates [5].

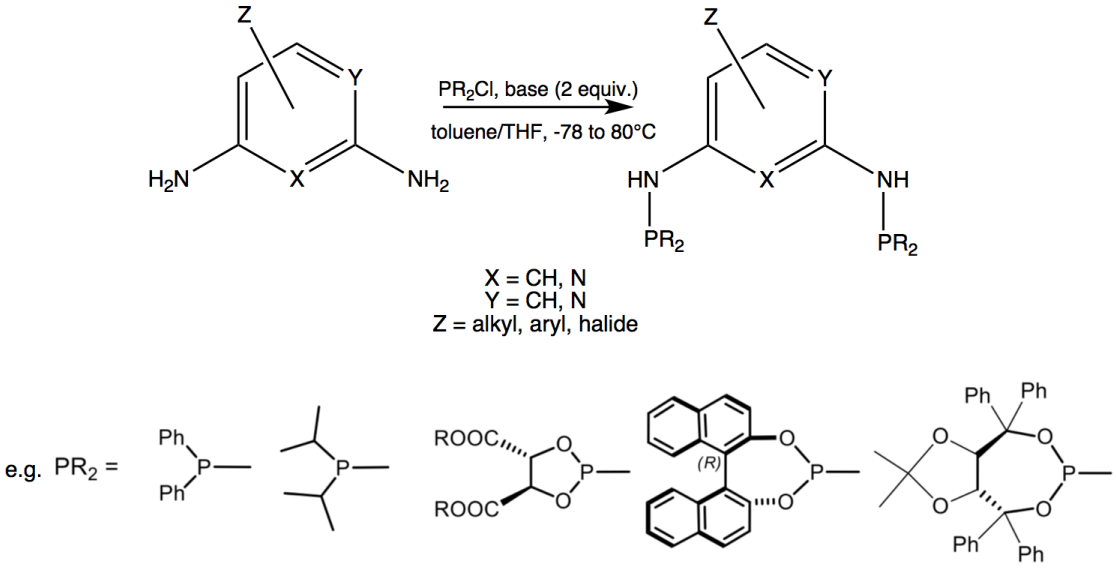

Figure 2.2: Synthesis of PNP pincer ligands, parts of this figure were taken from [5]

The synthetic route is shown in figure 2.2. P-N bonds are formed via condensation of primary or secondary amines and chlorophosphines in presence of a base. This method was first reported by Haupt and colleagues [22] and has been extended for PNPs [23] and PCPs [24].

3. CO Addition to Iron Complexes

This chapter takes strong reference from the work of Benito-Garragori et al. published in 2011 [25].

3.1 Introduction

The reactivity of transition-metals towards small molecules is an interesting topic in organometallic chemistry. The development of more sustainable chemistry depends on the incorporation of small molecules such as N_2, H_2, CO_2 or CO into complex chemicals.

To understand the bonding and the coordination properties of transition-metals to such small molecules typically the interactions of specific ligands with specific metal centers in different oxidation and spin states is examined. Thereby CO is often used as model ligand, because it is a mimic to N_2 and could help understand the reactivity regarding nitrogen fixation.

CO and iron in combination are linked to a number of industrial processes, such as the water-gas shift reaction and the Fischer-Tropsch reaction. Additionally the binding of CO to iron plays an important role in nature, e.g. the strong interaction of CO to iron in hemoglobin, which leads to an incapability of the molecule to absorb oxygen [26–29].

Since it was discovered that an Fe-CO moiety is present in the active site of hydrogenases the study of iron carbonyl compounds has increased [4, 30–38]. The carbonyl ligand generates some of the largest splitting of ligand field energy levels in transition-metal complexes. Coordination of CO therefore usually leads to a high-spin/low-spin crossover from S=2 or S=1 to S=0. High-spin, coordinatively unsaturated iron(II) complexes show different reactivities towards CO, ranging from very strong and irreversible to completely rejecting CO binding if spin-state changes are kinetically or thermodynamically unfavorable. Whether CO binding takes place or not depends on a number of factors: the number and nature of co-ligands (which determines the overall ligand field strength), the charge of the complex, the geometry of the complex and the spin-state of the metal center.

3.2 Spin-state Changes

The spin state of a complex if a given geometry is determined by the energy difference between the orbital splitting difference (ΔE, HOMO-LUMO gap) and the electron pairing energy (PE). The pairing energy is the energy required to pair up two electrons in one orbital. Whenever the energy difference ΔE of two or more orbitals is comparable to PE, different electron configurations with different spin states can be adopted. If ΔE>PE the low-spin state will be favored, is ΔE<PE the high-spin configuration will be preferred.

In general predictions about spin-state changes for each electronic configuration as a function of coordination number and geometry are easy. The overall ligand field strength naturally increases with an increasing coordination number. In first-row transition-metals the ligand field splitting is typically smaller than in second- and third-row transition-metals. Therefore coordinatively unsaturated iron complexes will favor a high-spin state.

In reactions, that involve open shell systems as starting material, intermediate or product, a spin state change will affect the thermodynamics or the kinetics of the reaction, since different spin states have different energies. Reactions, where a kinetic effect can result in a barrier that hinders the crossing between the spin states, are generally called "spin-blocked" or "spin-forbidden".

Spin state changes occur at the minimum energy crossing point (MECP). This corresponds to the lowest energy point at witch both the energy and the geometry of a molecule is the same on both the low-spin and the high-spin energy surface. Once a system reaches the MECP there is a certain possibility of "hopping" from one surface to the other, which means that the "spin-forbidden" reaction takes place [39, 40].

Figure 3.1 shows energy profiles for the coordination of CO to a coordinatively unsaturated metal complex ML_n ($16e^-$) resulting in a coordinatively saturated complex $ML_n(CO)$ ($18e^-$) with possible spin crossovers.

When $\Delta E \gg PE$ both the unsaturated starting complex and the saturated CO complex are existent in the same low-spin configuration. The reaction follows the same spin state surface S (figure 3.1a).

If the starting compound has a high-spin ground state there are three different possibilities: In the case described in figure 3.1b ΔE is bigger than PE and CO binding can still take place, if the MECP lies at low enough energies so that the energy gained by the reaction outweighs the loss of energy needed to reach the MECP. If the minimum energy crossing point is too high in energy the reaction will be "spin-blocked" and will not take place.

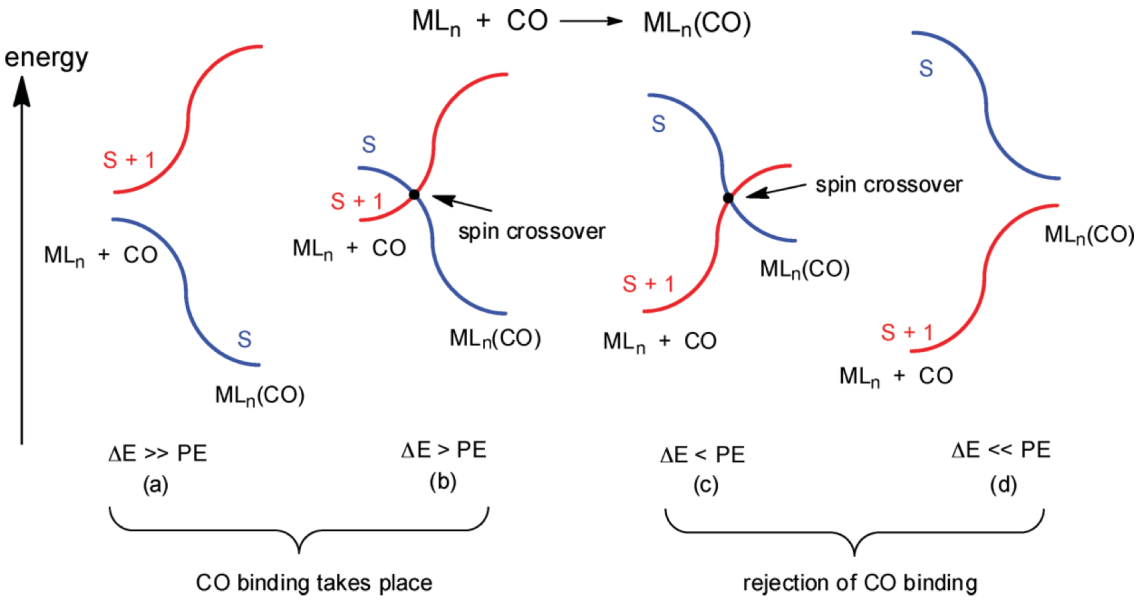

Figure 3.1: Energy profiles of the addition of CO to a coordinatively unsaturated complex in different spin states

In figures 3.1c and 3.1d the CO addition is thermodynamically disfavored. ΔE in figure 3.1c is smaller than PE and the system is more stable in the unsaturated high-spin state, CO addition will not take place.

The system will naturally also remain in the high-spin configuration, when ΔE is much smaller than PE like shown in figure 3.1d.

In this work the coordination of CO to Fe(PNP-*i*Pr)Cl_2 complexes was examined. Figures 3.2 and 3.3 show earlier described DFT calculations for the energy surfaces of these systems [25].

The *cis*-isomer (**1**) is formed in solid state despite of its thermodynamically slightly less stable state compared to the *trans*-product (**2**). Benito-Garagorri et al. explained this by the fact that in solid state the mobility is restricted due to the crystal packing. The formation of **2** requires more extreme changes in geometry than for **1**.

The DFT studies show that first the high-spin Fe(PNP)$COCl_2$ is formed when CO reacts with Fe(PNP)Cl_2. This high-spin species then undergoes a spin-crossover to yield the more stable low-spin complex.

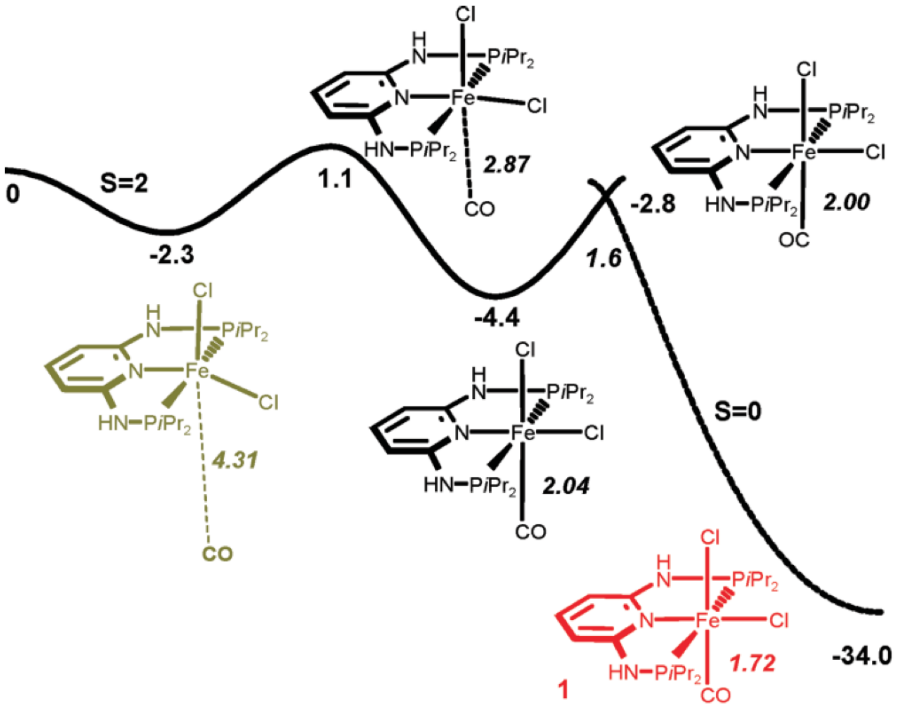

Figure 3.2: Energy profile (DFT/PBE) for the addition of CO to $Fe(PNP)Cl_2$ yielding *cis*-$[Fe(PNP)(CO)Cl_2]$ (**1**) (in the solid state)

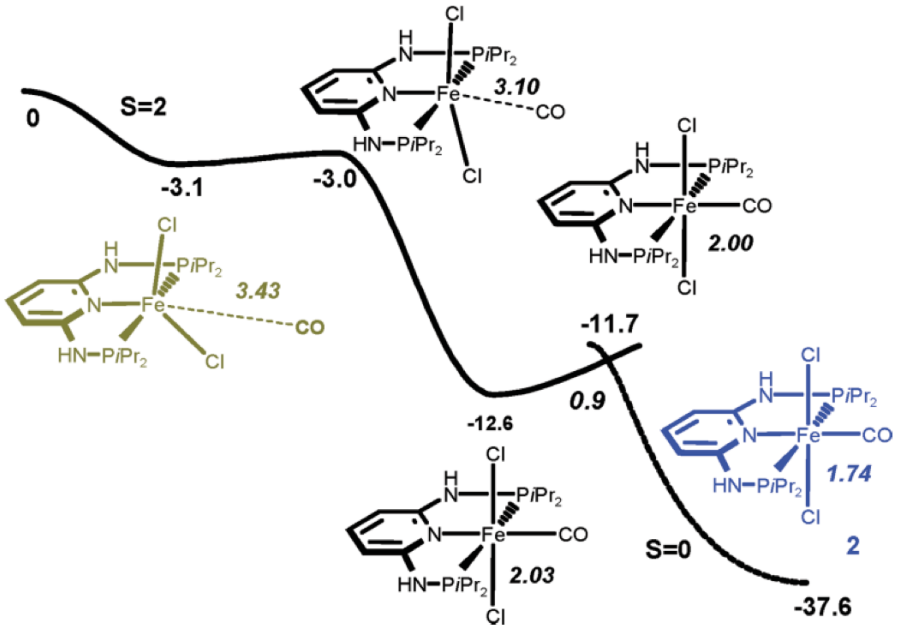

Figure 3.3: Energy profile (DFT/PBE) for the addition of CO to $Fe(PNP)Cl_2$ yielding *trans*-$[Fe(PNP)(CO)Cl_2]$ (**2**) (in solution)

4. Hydride Complexes in Catalysis

Many different pincer complexes have already been used in catalytic applications. The backbone is very robust and rigid and allows many structural modifications. Also it limits the number of active sites at the metal center, which ensures selectivity and stability of the catalyst.

Palladium pincer complexes mediate a number of catalytic reactions, mostly C-C bond forming reactions, ruthenium (II) PCP and NCN complexes have been effectively used in transfer hydrogenation reactions of ketones [41]. Dinuclear rhodium(III)-rhodium(I) PCP and NCN complexes have been used to catalyze the polymerization of phenylacetylene [42], several iridium(III) PCP pincer complexes have been found to catalyze alkane dehydrogenation [43], etc.

The contents of the following paragraphs are mostly taken from the short review of Gerald Bauer and Karl A. Kirchner published in 2011 [44].

The stereoselective hydrogenation of ketones with transition-metal catalysts to the corresponding enantiomerically pure alcohols is an important reaction in synthetic chemistry. Usually these hydrogenation reactions are catalyzed by complexes of precious metals such as rhodium, ruthenium or iridium [45, 46].

Ligand-metal bifunctional catalysis (metal-ligand cooperation) is often involved in these reactions [47–49], which means that as a result of heterolytic dihydrogen cleavage the complexes contain electronically coupled hydride ligands (blue in fig. 4.1) and acidic (red in fig. 4.1) hydrogen atoms (figure 4.1a). There are two possibilities for the reaction of these complexes with ketones shown in figure 4.1b and c. Either the groups can be transferred to the substrates in an outer-sphere mechanism (b) or by insertion of the substrate into the metal-H bond (c) [50].

Noble metals however are limited in availability, high in price and toxic for which reasons more attractive alternatives need to be found. The most obvious choice are iron complexes. Iron is the most abundant transition-metal in the Earth's crust. Even nature

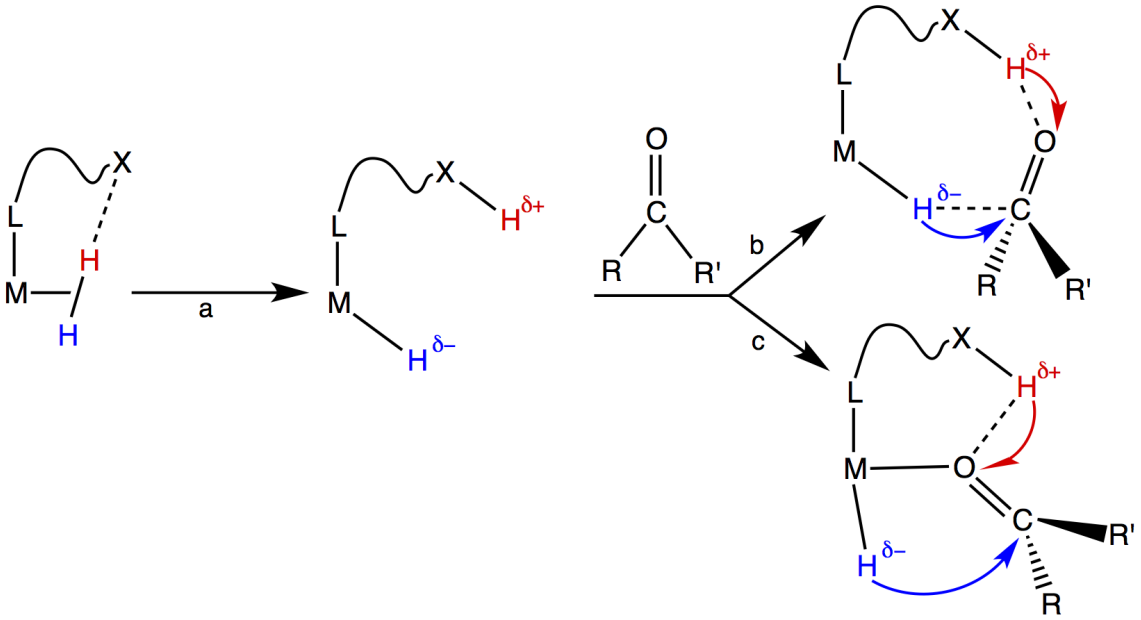

Figure 4.1: Key steps of catalytic hydrogenation of ketones to alcohols with a bifunctional catalyst

often uses iron-based catalysts for hydrogenation reactions [51, 52]. It is therefore not surprising that the preparation of well-defined iron catalysts of comparable activity to the noble metal catalysts is rapidly evolving field [53–57].

The first efficient iron catalyst for ketone hydrogenation was reported in 2007 [1]. Casey and Guan used the complex **1** shown in figure 4.2 originally prepared by Knölker et al. [58]. With complex **1** the reduction of ketones to alcohols can be accomplished under mild conditions with TON = 50 and with high chemo- and diastereoselectivity.

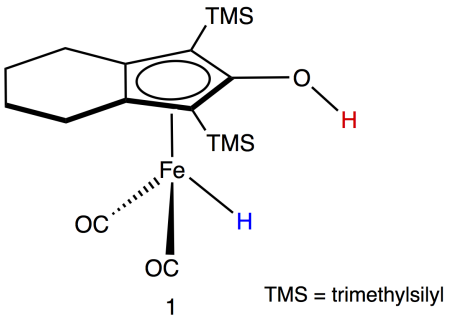

Figure 4.2: First efficient iron catalyst for hydrogenation of ketones

Two other iron complexes for catalytic hydrogenation of acetophenone have been prepared by Morris and co-workers [2,59]. Several dicationic iron complexes of the types *trans*-

$[Fe(MeCN)_2(Z\text{-}P_2N_2)](BF_4)_2$ and *trans*-$[Fe(MeCN)_2(Z\text{-}P_2N_2)](BF_4)_2$ have been used, where P_2N_2 can be various achiral and chiral ligands (figure 4.3).

For the first time an enantioselective hydrogenation could be achieved, but both the conversion (40%) and the enantioselectivity (27% *ee*) were only modest.

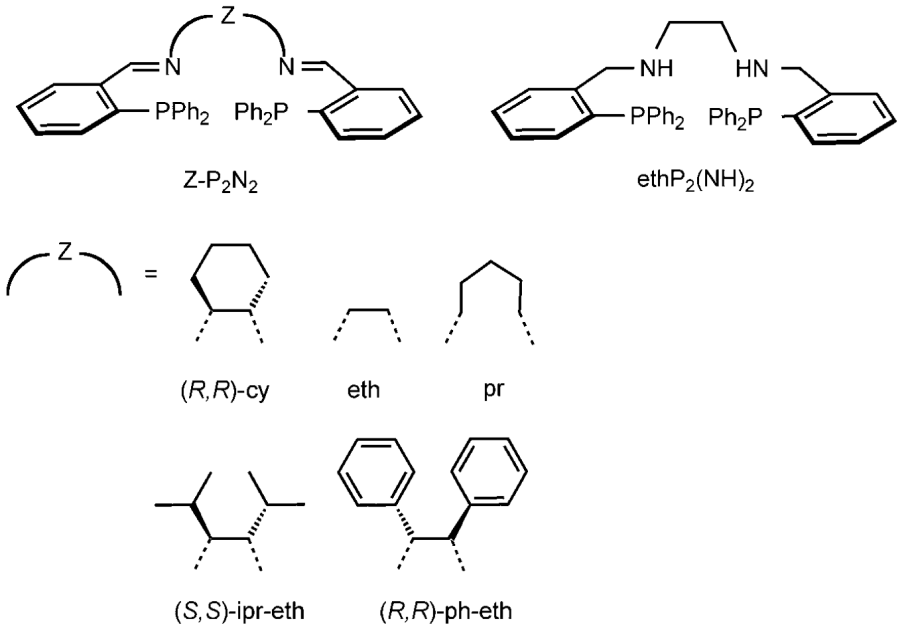

Figure 4.3: Examples of tetradentate P_2N_2 ligands

Monohydride iron(II) pincer complexes of the type [Fe(PNP-*i*Pr)Br(CO)H] (figure 4.4) have been reported by Milstein and co-workers in 2011 [3]. This is the most efficient well-defined bifunctional iron catalyst reported so far. The hydrogenation reaction takes place under mild conditions ($26 - 28\,^{\circ}C$) with turn over numbers up to 1880 (when 4.1 atm H_2 pressure is used).

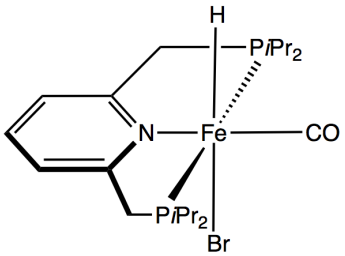

Figure 4.4: Monohydride iron(II) pincer complex developed by Milstein and co-workers

The disadvantage of these sorts of PNP complexes is their relatively difficult synthesis, that does not allow the easy introduction of chiral phosphines like in PNP ligands using aminophospine groups. On the other hand the NH-groups of the PNP ligands used in our research group seem to influence the reactivity and preparation of hydride complexes due to their high activity.

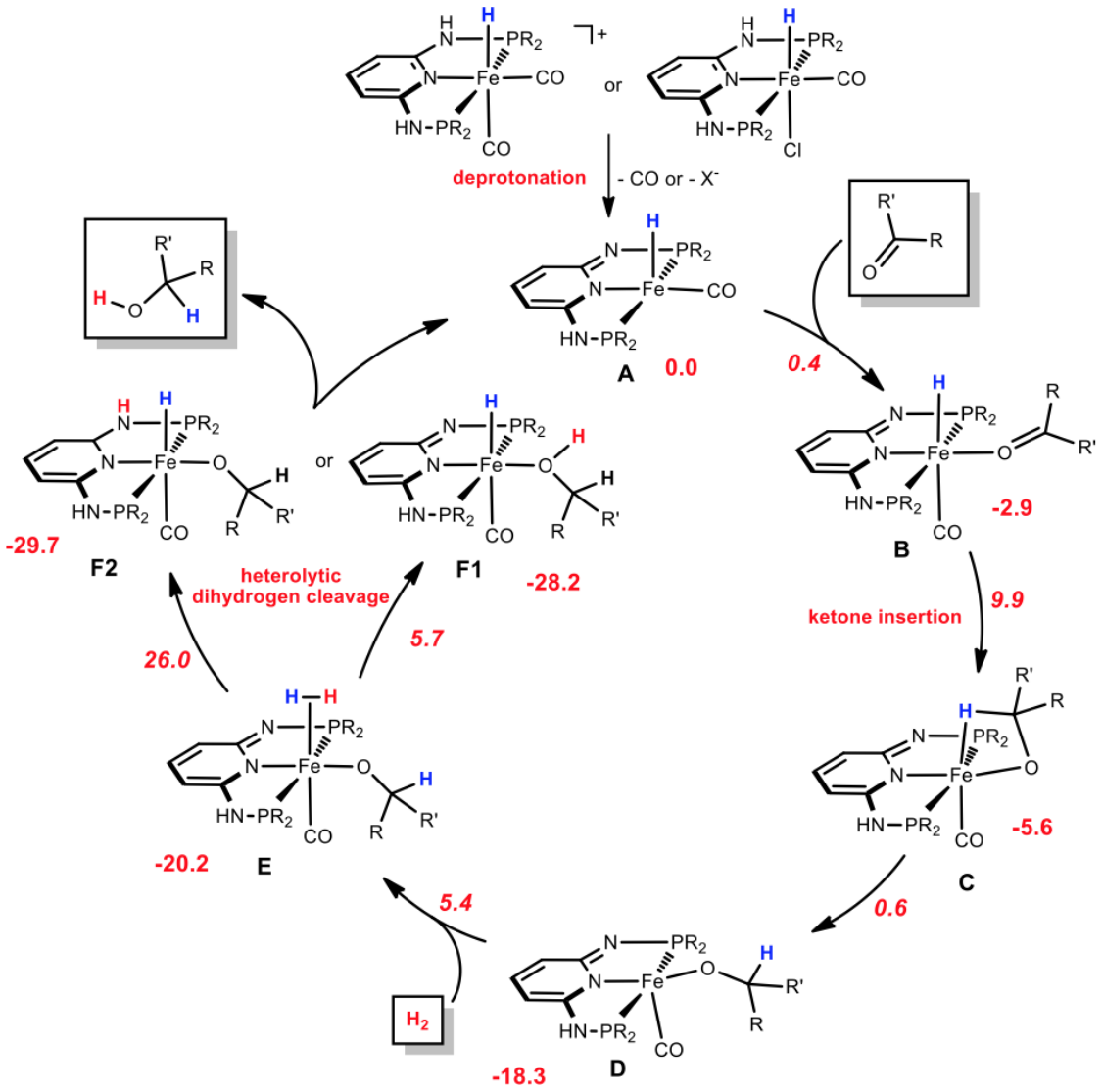

Figure 4.5: Proposed catalytic cycle for the hydrogenation of ketones to alcohols catalyzed by [Fe(PNP-*i*Pr)Cl(CO)H]

Figure 4.5 shows the proposed catalytic cycle for the hydrogenation of ketones to alcohols catalyzed by [Fe(PNP-*i*Pr)Cl(CO)H]. The catalytically active species is formed

after deprotonation and dearomatization of the precursor to yield a pentacoordinated $16e^-$ species **A**. To this complex the ketone can coordinate (**B**) followed by its insertion into the iron-H bond (**C**) to give the alkoxide complex **D**. This intermediate readily adds H_2 (**E**), which can then be heterolytically cleaved to give either **F1** or **F2**. The activation energies calculated and listed in figure 4.5 show, that formation of **F1** is more likely. The catalytic cycle is closed upon elimination of the desired alcohol, whereby the starting species **A** is regained.

Part II

RESULTS AND DISCUSSION

5. Ligands

5.1 Introduction

Transition metal complexes are important tools for synthetic chemists [5]. A simple way to modify the properties of transition metal complexes is via their ligands, such as pincer ligands. Those tridentate ligands have good stability, activity and variability. The first pincer complexes were synthesized in the 1970s [15], but only in the 1990s several applications were found, for example catalysts in C-C bond forming reactions, polymerization reactions, transfer hydrogenation and dehydrogenation reactions [20, 21].

In this work known PNP pincer ligands (**1a**, **1b**, **2b** and **3c**) as well as new ones (**2a**, **3b**, **4b** and **4c**) were synthesized via a modular synthetic route, which allows the use of many different substrates to give ligands with different properties, e.g. chirality.

The aminophosphine groups used allow to introduce various different phosphines by condensation reaction of aromatic diamines and electrophilic chlorophosphines [5].

5.2 PNP Ligands

Synthesis

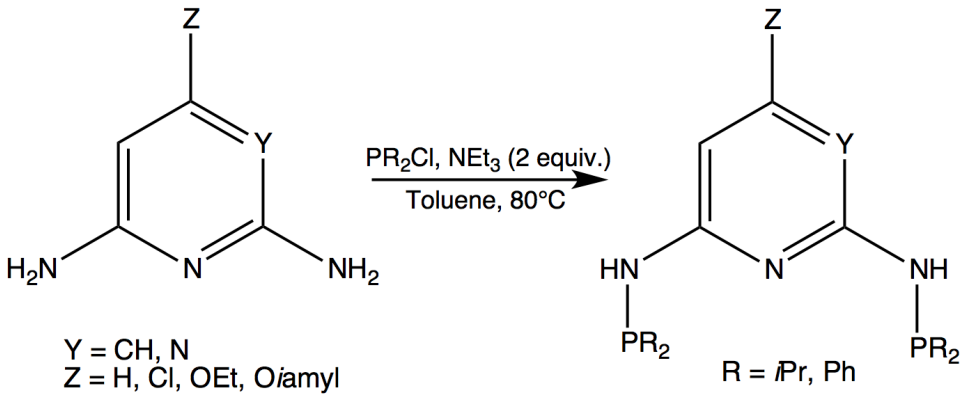

Figure 5.1: PNP ligand synthesis

The synthesis of PNP ligands was conducted according to literature [5].

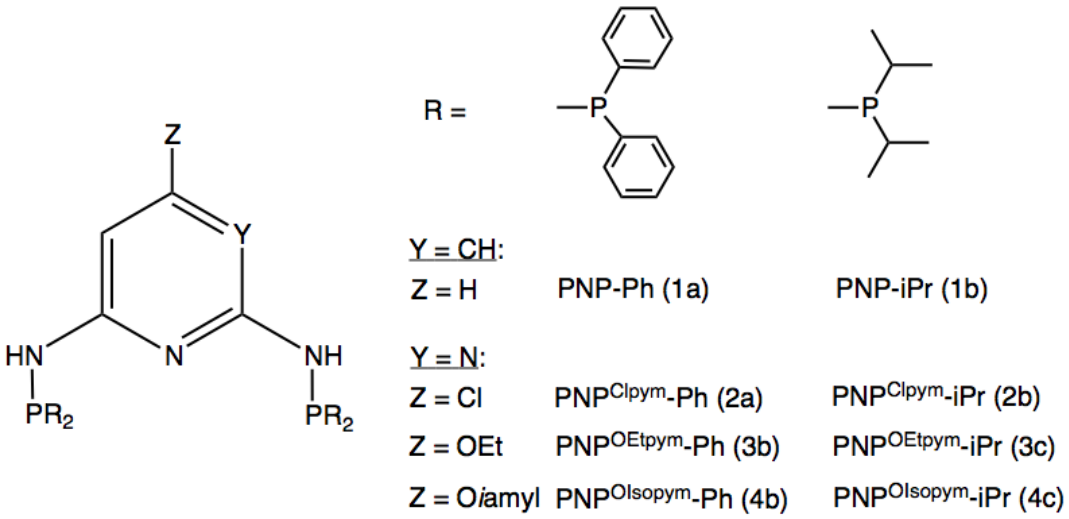

Figure 5.2: different PNP ligands

To a suspension of 2,6-diaminopyridine or the respective 2,6-diaminopyrimidine in toluene 2 equivs of NEt_3 were added and the mixture was cooled to 0 °C. Then 2 equivs of the corresponding chlorophosphine were added dropwise. The reaction was heated to 80 °C and stirred at that temperature for 12h. Thereby a precipitate of $NEt_3 \cdot HCl$ was formed, which was filtered off after the reaction was completed. The solvent was removed under vacuum and the ligands were obtained in moderate to excellent yields (55-96%) as white solids.

Using this procedure the PNP ligands **1a**, **1b**, **2a**, **2b**, **3b**, **3c**, **4b** and **4c** were synthesized. Many other achiral and chiral chlorophosphines can be used in the same way. Chiral precursors would lead to chiral PNP ligands, which are interesting for enantioselective reactions.

The precursors for the pyrimidine based ligands **3b**, **3c**, **4b** and **4c** were prepared using 2,6-diamino-4-chloro-pyrimidine as starting material [60].

Two equivs of NaH were added to an excess of ethanol or isoamyl alcohol to give the alkoxide, to which the 2,6-diamino-4-chloro-pyrimidine was added. The mixture was refluxed for 12h, after which the solvent was removed under reduced pressure to give the substituted 2,6-diaminopyrimidines as white solids. Both precursors could be obtained in very good yields (78-86%).

Using this procedure the precursors **3a** and **4a** were synthesized. It was also tried to react propargylic alcohol with 2,6-diamino-4-chloro-pyrimidine in different ways to give an alkyene functionalized ligand for immobilization of the complexes on surfaces, but no reaction could be found that yielded the desired product.

Characterization

The ligands and precursors were all characterized by ^{1}H, ^{31}P$\{^{1}$H$\}$ and ^{13}C$\{^{1}$H$\}$ NMR spectroscopy. The progress of the reaction can be monitored using ^{31}P$\{^{1}$H$\}$ NMR spectroscopy. Ligands **1a** and **1b** and the starting materials exhibit a single peak, whereas ligands **2a**, **2b**, **3b**, **3c** and **4b** show two singlets and ligand **4c** gives rise to a broad singlet. The signals of the ligands are shifted to higher fields compared to the chlorophosphines. Moreover, the signals for the ligands bearing isopropyl groups are shifted to lower fields than the ones with phenyl substituents. Table 5.1 shows the ^{31}P$\{^{1}$H$\}$ shifts for each ligand.

Table 5.1: ^{31}P$\{^{1}$H$\}$ NMR shifts of PNP ligands

	PNP	PNP^{Clpym}		PNP^{OEtpym}		PNP^{OIsopym}	
Ph	37.8	39.6	37.6	37.9	37.6	37.9	37.3
*i*Pr	60.4	62.9	60.3	61.6	60.5	60.1	

The ^{1}H and ^{13}C$\{^{1}$H$\}$ NMR show the peaks in the expected areas.

6. Complexes

6.1 Introduction

The development of new iron-based catalysts for the hydrogenation of ketones is an important topic in organometallic chemistry. Especially the stereoselective hydrogenation of ketones to the corresponding enantiomerically pure alcohols is a key step in the synthesis of, e.g., pharmaceuticals and fine chemicals [44].

Many transition metal complexes containing noble metals such as rhodium, ruthenium or iridium are known to catalyze this reactions [45,46]. However noble metals are available only in limited quantities, are expensive and toxic. That is why environmentally friendly and more economical alternatives need to be found.

Iron-based catalysts of comparable activity would be a cheaper and cleaner way to catalyze those reactions. Some efficient iron catalysts have already been reported [1,2,59, 61,62].

In all these cases strong-field tridentate or tetradentate ligands and sometimes CO ligands are required so that the iron center can maintain a low spin state [44].

The complexes synthesized in the course of this work all bear easily modifiable tridentate PNP pincer ligands described in chapter 5. This allows the facile introduction of chiral components to give eventually stereoselective hydrogenation catalysts.

6.2 Fe(PNP-*i*Pr)Cl_2 Complexes

Synthesis

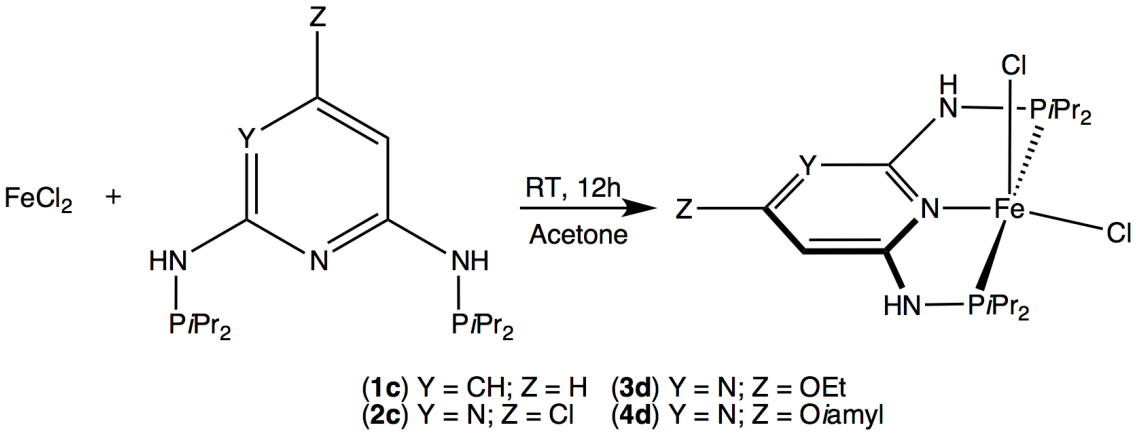

Figure 6.1: Synthesis of Fe(PNP-*i*Pr)Cl_2 complexes

The Fe(PNP-*i*Pr)Cl_2 complexes were synthesized according to the literature [63].

To a suspension of anhydrous $FeCl_2$ in acetone one equiv of the PNP-*i*Pr ligand was added. The mixture was stirred for 12h. Thereby, depending on the ligand, a white to yellow solid formed. The solvent was removed under reduced pressure and the paramagnetic complexes were obtained in very good yields (94-99%). The synthesis also worked when THF or CH_3NO_2 were used as solvents.

Using this procedure the complexes **1c**, **2c**, **3d** and **4d** could be obtained. This reaction could only be conducted with the PNP-*i*Pr ligands **1b**, **2b**, **3c** and **4c**. When PNP-Ph ligands were used in the same reaction, it resulted in different complexes shown in chapter 6.5.

All these complexes synthesized via this route are air stable in both solid state and solution for several days.

Characterization

Due to their paramagnetic behavior the complexes could only be characterized using ^{1}H NMR spectroscopy, which resulted in the same signals already described in literature [64]. The new complex **4d** showed very similar signals with the C*H* groups of the isopropyl moieties shifted to the lowest and the protons of the isoamyl chain at the highest fields.

Complexes **2c** and **4d** was also characterized by X-ray crystallography, whereas the structure of **2c** was already described in literature [64] and is shown in figure 6.2. The crystals of **4d** were grown by slow diffusion of diethyl ether into a concentrated solution of the complex in THF (Figure 6.3). The complex is bridged via N-H$\cdots$Cl hydrogen bonds to four neighboring complexes. Because of the long and flexible isoamyl chain and the two possible positions for the pyrimidine ring the obtained crystals showed defects, which lead to a poor structure.

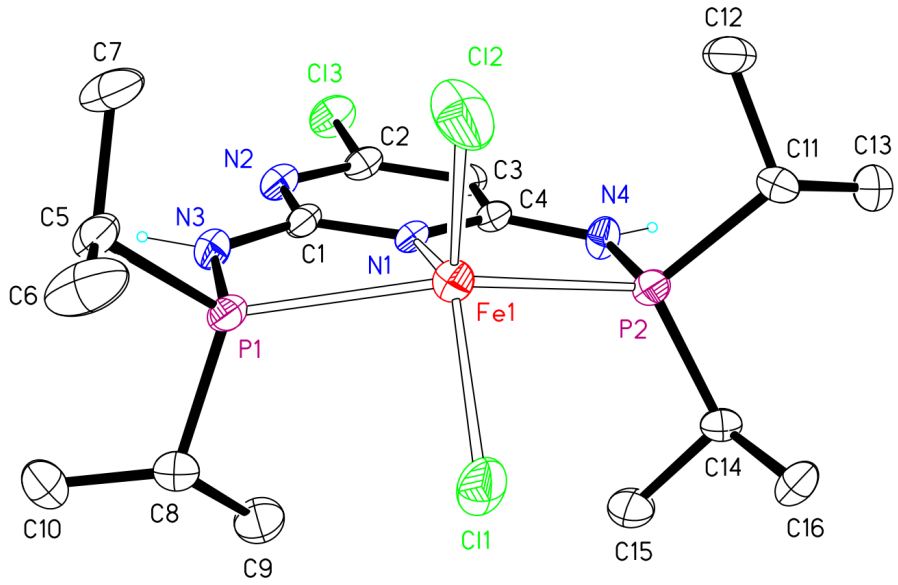

Figure 6.2: ORTEP plot of Fe(PNP^{Clpym}-iPr)Cl$_2$ **2c** showing 50% thermal ellipsoids (C-bound H atoms are omitted for clarity)

Selected bond lengths (Å) and angles (deg): Fe-P(1) 2.4904(12), Fe-P(2) 2.5188(12), Fe-N(1) 2.270(3), Fe-Cl(1) 2.4200(12), Fe-Cl(2) 2.2601(4); Cl(1)-Fe-Cl(2) 110.21(6), P(1)-Fe-P(2) 146.20(4).

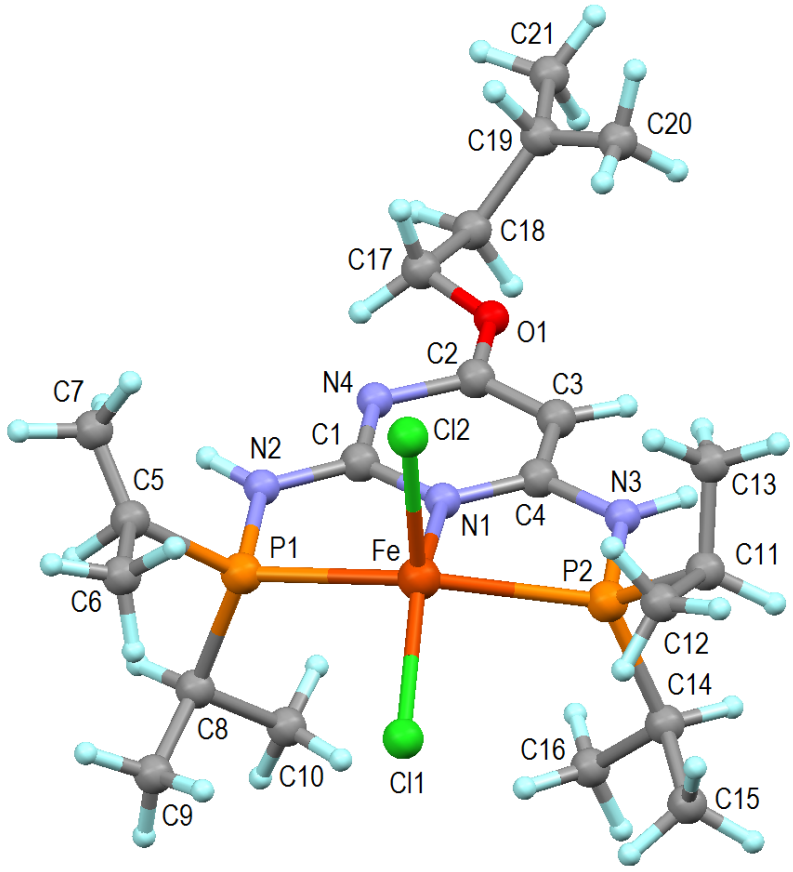

Figure 6.3: Molecular structure of Fe(PNP^{OIsopym}-*i*Pr)Cl_2 **4d**

Selected bond lengths (Å) and angles (deg): Fe-P(1) 2.468(3), Fe-P(2) 2.454(2), Fe-N(1) 2.205(6), Fe-Cl(1) 2.357(2), Fe-Cl(2) 2.310(2), P(1)-N(2) 1.688(9), P(2)-N(3) 1.695(8), P(1)-C(5) 1.806(11), P(1)-C(8) 1.858(15), P(2)-C(11) 1.728(15), P(2)-C(14) 1.855(17), O(1)-C(2) 1.332(12), O(1)-C(17) 1.27(3), N(1)-C(1) 1.372(12), N(1)-C(4) 1.342(13), N(4)-C(1) 1.359(13), N(4)-C(2) 1.366(16), C(2)-C(3) 1.321(15), C(3)-C(4) 1.327(12); Cl(1)-Fe-Cl(2) 111.29(8), P(1)-Fe-P(2) 146.03(11).

6.3 Fe(PNP-*i*Pr)(CO)Cl_2 Complexes

Synthesis

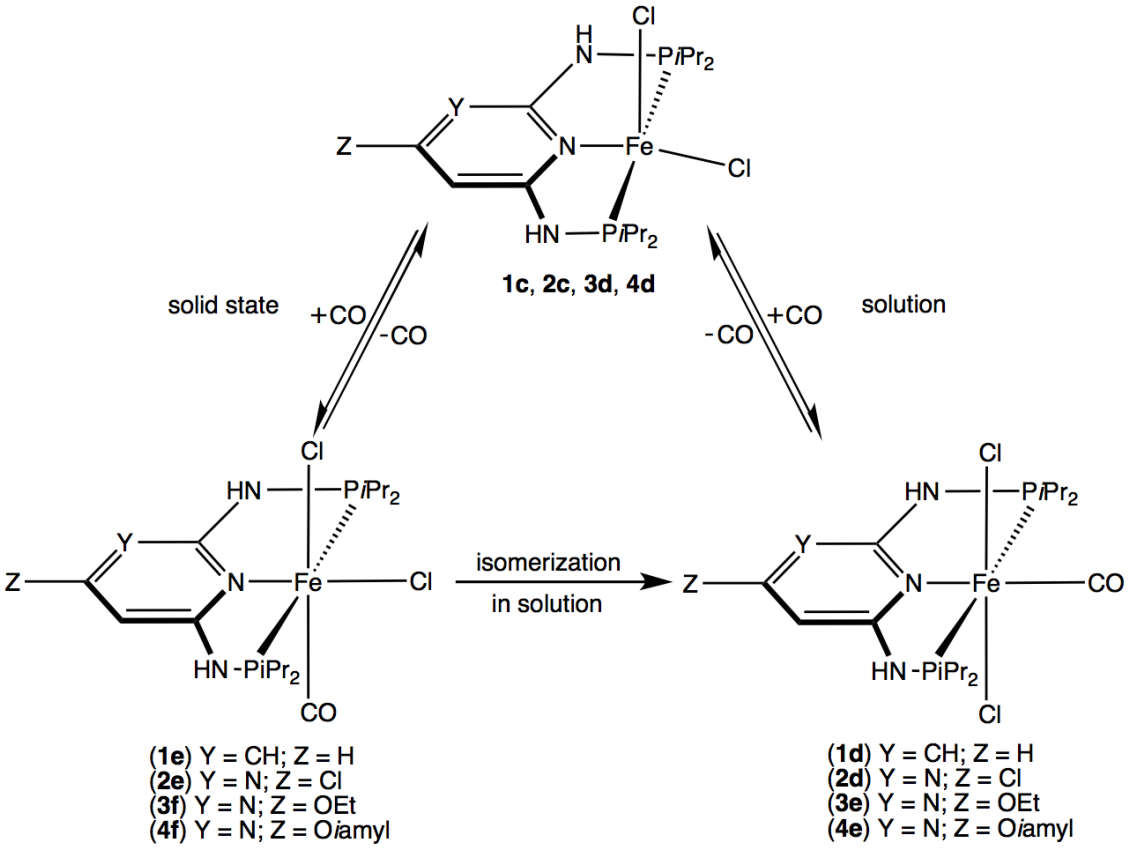

Figure 6.4: Synthesis of Fe(PNP)(CO)Cl_2 complexes

The *cis*- and *trans*-Fe(PNP)(CO)Cl_2 complexes **1d**, **1e**, **2d**, **2e**, **3e**, **3f**, **4e** and **4f** were synthesized according to literature [64, 65].

***trans*-Fe(PNP-*i*Pr)(CO)Cl_2** was synthesized by bubbling CO through a solution of the corresponding Fe(PNP)Cl_2 complex in acetone or THF. The progress of the reaction could be observed through the color change from white or yellow to violet or blue. The solvent was then removed under reduced pressure to give the complexes **2d**, **3e** and **4e** as violet solids and **1d** as blue solid in excellent yields (95%-99%).

These complexes are air stable in solid state and in solution for several days. After some time they begin to lose the CO ligand, when they are not stored under argon or CO atmosphere.

CO was passed over a solid sample of the Fe(PNP)Cl_2 complexes to give ***cis*-Fe(PNP-**

***i*Pr)(CO)Cl$_2$**. During the reaction the color changed from white or yellow to red. The complexes **1e**, **2e**, **3f** and **4f** could all be obtained with 100% yield as deep red solids.

The *cis*-complexes are relatively stable in solid state, but lose the CO ligands much faster than the *trans*-complexes. In solution very fast isomerization to the *trans*-complexes can be observed.

Characterization

The *trans*-Fe(PNP-*i*Pr)(CO)Cl$_2$ complexes were characterized by ^{1}H, ^{31}P{^{1}H} and ^{13}C{^{1}H} NMR spectroscopy. ^{31}P{^{1}H} spectra of **1d** and **1e** show single peaks, all the other complexes show two doublets due to the coupling of the two chemically different phosphor atoms. Table 6.1 shows the obtained ^{31}P{^{1}H} shifts and the coupling constant for all complexes.

The ^{1}H and ^{13}C{^{1}H} NMR spectra show the peaks in the expected areas. The CO peak in the ^{13}C{^{1}H} NMR appears as triplet at very low fields (221-225 ppm).

The *cis*-Fe(PNP-*i*Pr)(CO)Cl$_2$ complexes could only be characterized by ^{1}H and ^{31}P{^{1}H} NMR spectroscopy due to their very fast isomerization to the *trans*-complexes. The ^{1}H spectra are often very hard to analyze depending on the rate of isomerization. All peaks appear as singlets and are not integrable because of the fast isomerization reaction in solution. Based on these results it was refrained from measuring ^{13}C{^{1}H} NMR spectra as they would not yield the desired peaks but rather the ones belonging to the *trans*-species.

Table 6.1: ^{31}P{^{1}H} NMR shifts of Fe(PNP-*i*Pr)(CO)Cl$_2$ complexes

	PNP	PNP^{Clpym}	PNP^{OEtpym}	PNP^{OIsopym}
trans	133.1	142.5 128.0	138.8 126.2	140.0 127.0
J		177 Hz	177 Hz	179 Hz
cis	117.3	126.8 113.5	123.9 112.4	123.7 112.0
J		210 Hz	234 Hz	206 Hz

Due to the presence of carbonyl groups IR-spectroscopy was also used to characterize the complexes **1d**, **1e**, **2d**, **2e**, **3e**, **3f**, **4e** and **4f**. The wave numbers obtained are summarized in table 6.2.

Molecular structures of **1d** and **2d** was already described in literature [64, 65]. Figure

Table 6.2: CO stretching bonds of Fe(PNP-*i*Pr)(CO)Cl_2 complexes

	PNP	PNP^{Clpym}	PNP^{OEtpym}	$PNP^{OIsopym}$
trans	1956	1972	1958	1967
cis	1947	1958	1955	1956

6.5 shows the structure of **2d**. Crystallization experiments for **3e** and **4e** so far yielded highly disordered crystals that were not suitable for X-ray crystallography. Because of the fast isomerization of the *cis*-complexes no molecular structures could be obtained.

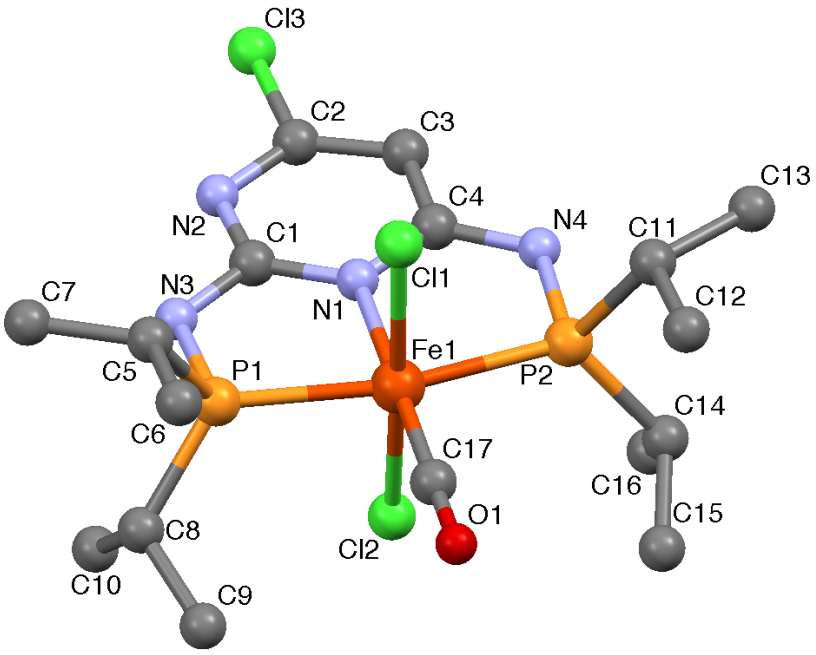

Figure 6.5: Molecular structure of Fe(PNP^{Clpym}-*i*Pr)(CO)Cl_2 **2d** (solvent molecules and H atoms are omitted for clarity)

Selected bond lengths (Å) and angles (deg): Fe-P(1) 2.2546(5), Fe-P(2) 2.2469(5), Fe-N(1) 1.9890(14), Fe-Cl(1) 2.3304(5), Fe-Cl(2) 2.3067(5), Fe-C(17) 1.7659(18); Cl(1)-Fe-Cl(2) 175.36(2), P(1)-Fe-P(2) 166.74(2), N(1)-Fe-C(17) 178.98(7).

6.4 $[Fe(PNP\text{-}iPr)(CO)_2Cl]^+$ Complexes

Synthesis

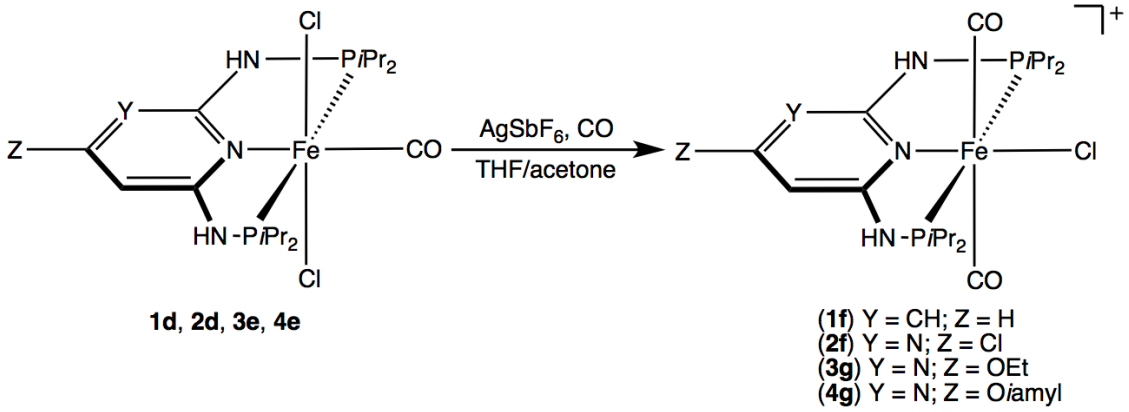

Figure 6.6: Synthesis of $Fe(PNP\text{-}iPr)(CO)_2Cl]^+$ complexes

The $[Fe(PNP\text{-}iPr)(CO)_2Cl]^+$ complexes were prepared according to literature [66].

To a solution of either *cis*- or *trans*-$Fe(PNP\text{-}iPr)(CO)Cl_2$ or $Fe(PNP\text{-}iPr)Cl_2$ in THF or acetone one equiv of $AgSbF_6$ was added as chloride scavenger in the presence of CO. The reaction mixture was stirred for 30 minutes and the precipitate of AgCl was filtered of. The solvent was removed under reduced pressure to give the products as red solids in good yields (83%-94%).

The complexes with PNP-*i*Pr and PNP^{OEtpym}-*i*Pr as ligands (**1f** and **3g**) the reaction resulted in pure product composed only of the *trans*-$Fe(PNP\text{-}iPr)(CO)_2Cl]^+$ species, whereas the complexes with PNP^{Clpym}-*i*Pr and $PNP^{OIsopym}$-*i*Pr (**2f**/**2g** and **4g**/**4h**) yielded in mixtures of the *cis*- and *trans*-products.

It was also tried to use $Fe(PNP^{Clpym}\text{-}Ph)(CO)Cl_2$ as starting material, which was the only PNP-Ph complex to give a pure precursor, but the reaction yielded a mixture of *cis*- and *trans*-species and in addition $[Fe(PNP^{Clpym}\text{-}Ph)_2Cl]^+$(see chapter 6.5).

Characterization

All complexes were characterized by ^1H, $^{31}P\{^1H\}$ and $^{13}C\{^1H\}$ NMR spectroscopy. The ^1H NMR spectra all show the expected peaks, but the ones of the mixtures **2f**/**2g** and **4g**/**4h** only show broad single peaks in the expected areas. $^{13}C\{^1H\}$ NMR spectroscopy gave the expected shifts similar to the free ligands and additionally the CO ligands, which

both appear at the same resonance.

The molecular structure of *trans*-[Fe(PNP-*i*Pr)$(CO)_2$Cl]$^+$ (as the $CF_3SO_3^-$ salt) was described in literature [66] and is shown in figure 6.7. Once again it was not possible to obtain measurable single crystals of the complexes with pyrimidine-based ligands due to their high disordering.

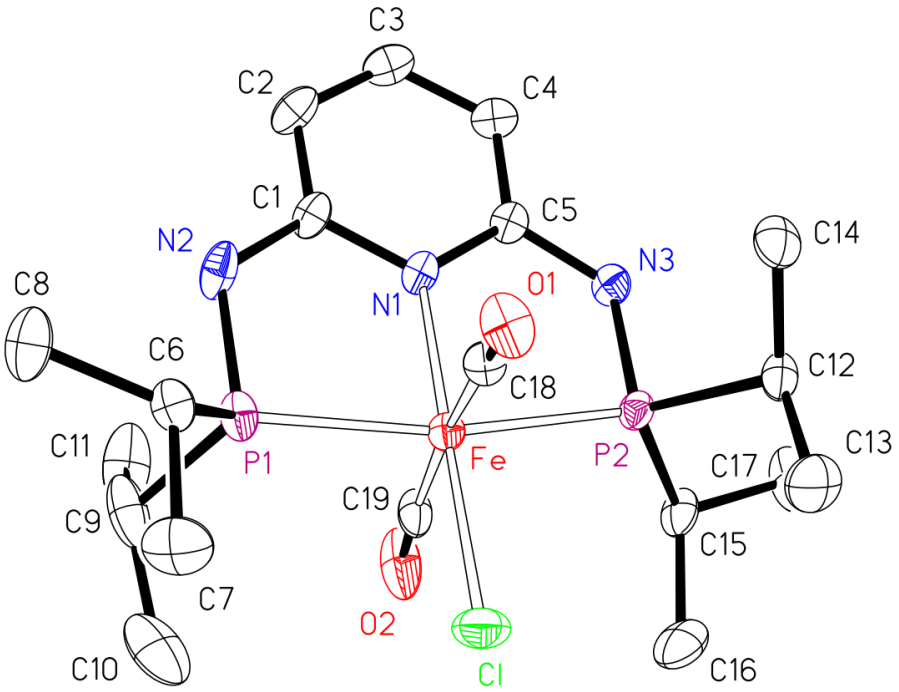

Figure 6.7: ORTEP plot of [Fe(PNP-*i*Pr)$(CO)_2$Cl]$^+$ **1f** showing 50% thermal ellipsoids (solvent molecules and H atoms are omitted for clarity)

Selected bond lengths (Å) and angles (deg): Fe-P(1) 2.2557(9), Fe-P(2) 2.2558(9), Fe-N(1) 1.987(3), Fe-Cl 2.3019(10), P(1)-N(2) 1.692(3), P(2)-N(3) 1.692(3), N(2)-C(1) 1.368(4), N(3)-C(5) 1.369(4), P(1)-C(6) 1.855(3), P(1)-C(9) 1.846(4), P(2)-C(12) 1.844(3), P(2)-C(15) 1.853(3); C(18)-Fe-C(19) 171.34(16), C(18)-Fe-N(1) 94.86(13), C(19)-Fe-N(1) 93.79(13), N(1)-Fe-Cl 178.22(8), P(1)-Fe-P(2) 167.80(3).

6.5 $[Fe(PNP\text{-}Ph)_2Cl]^+$ Complexes

Synthesis

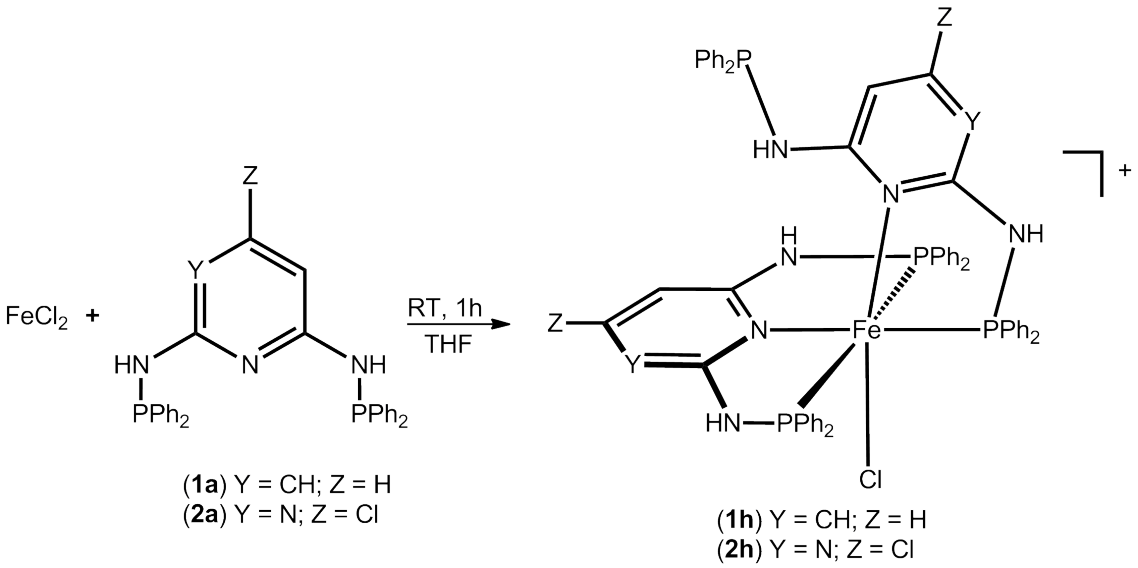

Figure 6.8: Synthesis of $[Fe(PNP\text{-}Ph)_2Cl]^+$ complexes

The synthesis of these complexes was conducted by reacting one equiv of $FeCl_2$ with two equivs of the corresponding PNP-Ph ligand for 1h in THF. To change the counterion from chloride to BF_4^-, 4 equivs of $NaBF_4$ were added to the reaction mixture. The precipitate was then filtered off and the remaining green solution was evaporated to give the products as green solids in good yields (95%).

When PNP^{OEtpym}-Ph **3b** and $PNP^{OIsopym}$-Ph **4b** were used as ligands similar complexes could be obtained, but the dangling aminophosphine arm of the κ^2-bound ligand was missing like shown in figure 6.9. The dangling arm is prone to hydrolysis and traces of water in solvents lead to P-N bond cleavage.

Characterization

The obtained complexes **1h** and **2h** were characterized by ^1H, $^{31}P\{^1H\}$ and $^{13}C\{^1H\}$ NMR spectroscopy, whereas the compound **2h** showed two different isomers **A** and **B** (figure 6.10). The ^1H NMR shows signals in the expected areas. The NH protons each give an own signal, the one on the dangling arm giving a doublet, but the protons of the phenyl groups and the ones of the pyrimidine rings only give broad singlet peaks.

The $^{31}P\{^1H\}$ NMR is shown in figure 6.12 for complex **2h**. The three phosphor coordinated to the iron center are shifted to lower fields compared to the free ligand and

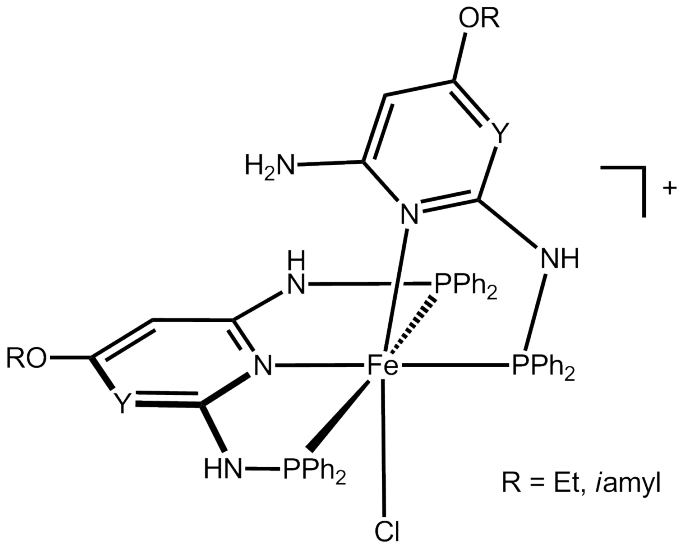

Figure 6.9: $[Fe(PNP\text{-}Ph)_2Cl]^+$ complexes without the aminophosphine arm

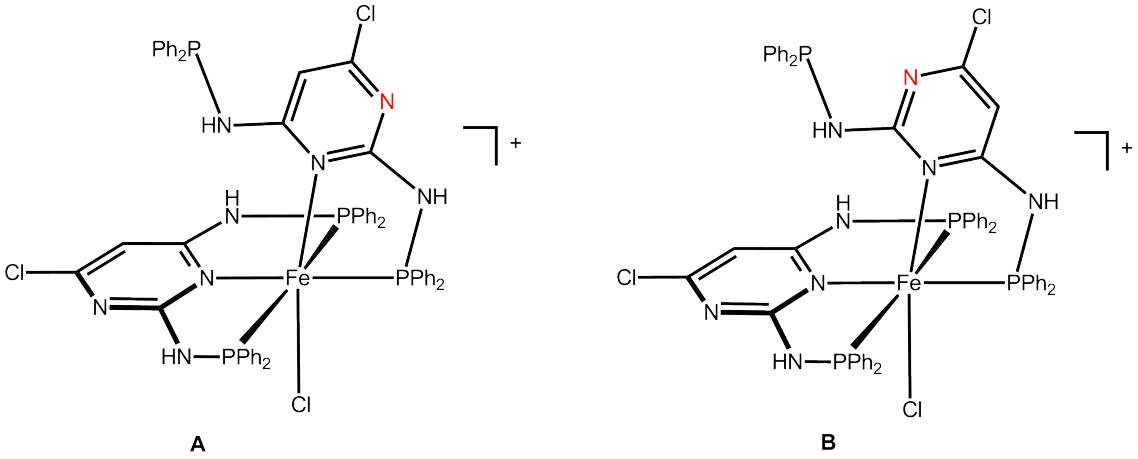

Figure 6.10: Two different isomers are possible with pyrimidine ligand bearing complexes

give two doublet on doublets and one triplet. The phosphor of the dangling arm gives a singlet with similar chemical shift as the free ligand. Two different isomers are obtained in this reaction, which can easily be seen in the $^{31}P\{^1H\}$ NMR spectrum. It could not be determined, which isomer corresponds to the unmarked signals and which to the signals marked with a red star in figure 6.12.

Complex **1h** was also characterized by X-ray crystallography. The crystals were grown by slow diffusion of diethyl ether into a concentrated solution of the complex in THF (figure 6.11). It can easily be seen, that one of the ligands is coordinated in a κ^3 fashion and the other one in κ^2. The crystals are a solvate with two well-ordered THF solvent molecules

hydrogen bonded to NH-groups. A third solvent molecule, not hydrogen bonded to NH, was badly disordered and is thought from its elongated shape to be an Et_2O molecule. Due to its disorder, this solvent molecule was squeezed with program PLATON. Also affected by this solvent disorder is the BF_4 anion. As no reasonable disorder model could be constructed, the BF_4 anion was refined as a single moiety with partly very large anisotropic displacement ellipsoids. The BF_4^- anion is hydrogen bonded to one of the NH-groups of the Fe complex.

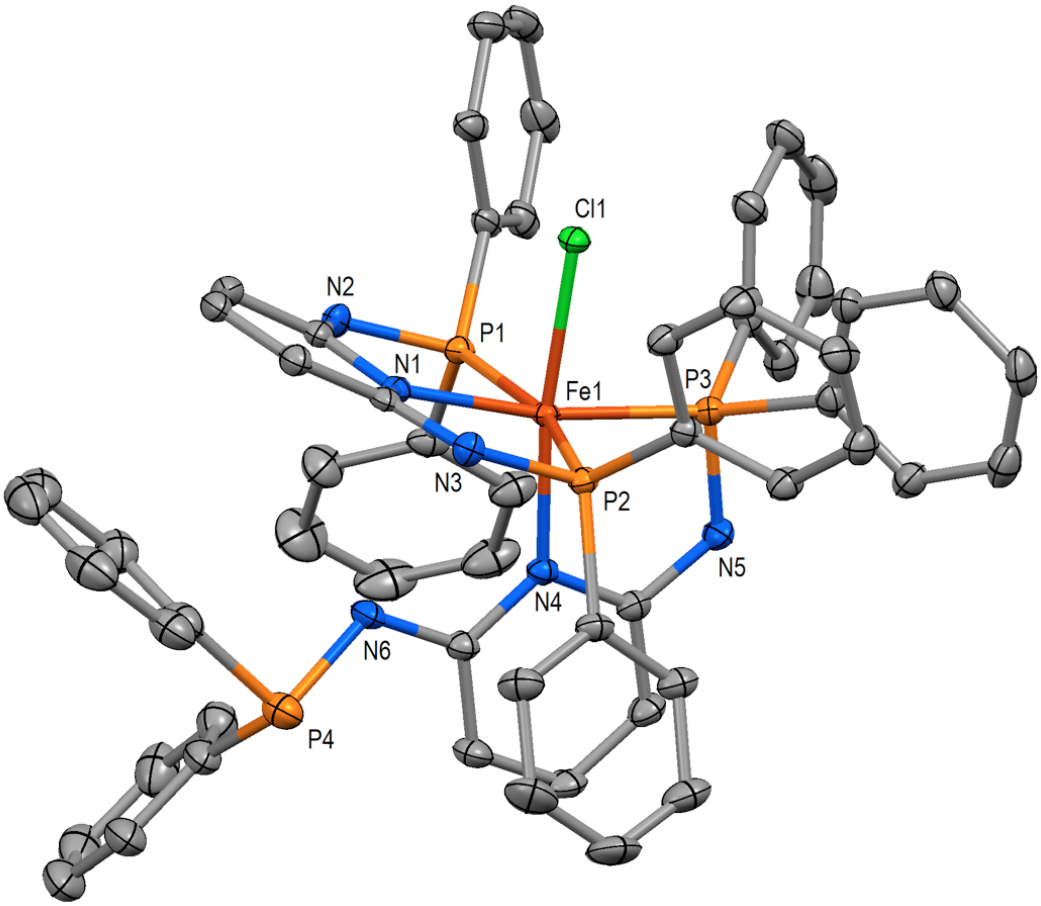

Figure 6.11: ORTEP plot of $[Fe(PNP\text{-}Ph)_2Cl]^+$ **1h** showing 50% thermal ellipsoids (solvent molecules and H atoms are omitted for clarity)

Selected bond lengths (Å) and angles (deg): Fe-P(1) 2.2439(7), Fe-P(2) 2.2530(7), Fe-P(3) 2.1845(7), Fe-N(1) 2.064(2), Fe-N(4) 2.084(3), Fe-Cl(1) 2.3330(7), P(1)-N(2) 1.693(2), P(2)-N(3) 1.692(2), P(3)-N(5) 1.679(2), P(4)-N(6) 1.742(2); P(1)-Fe-P(2) 163.33(3), N(4)-Fe-Cl 172.36(6), P(3)-Fe-N(1) 170.02(6), N(1)-Fe-Cl 81.43(6), N(1)-Fe-N(4) 105.91(8).

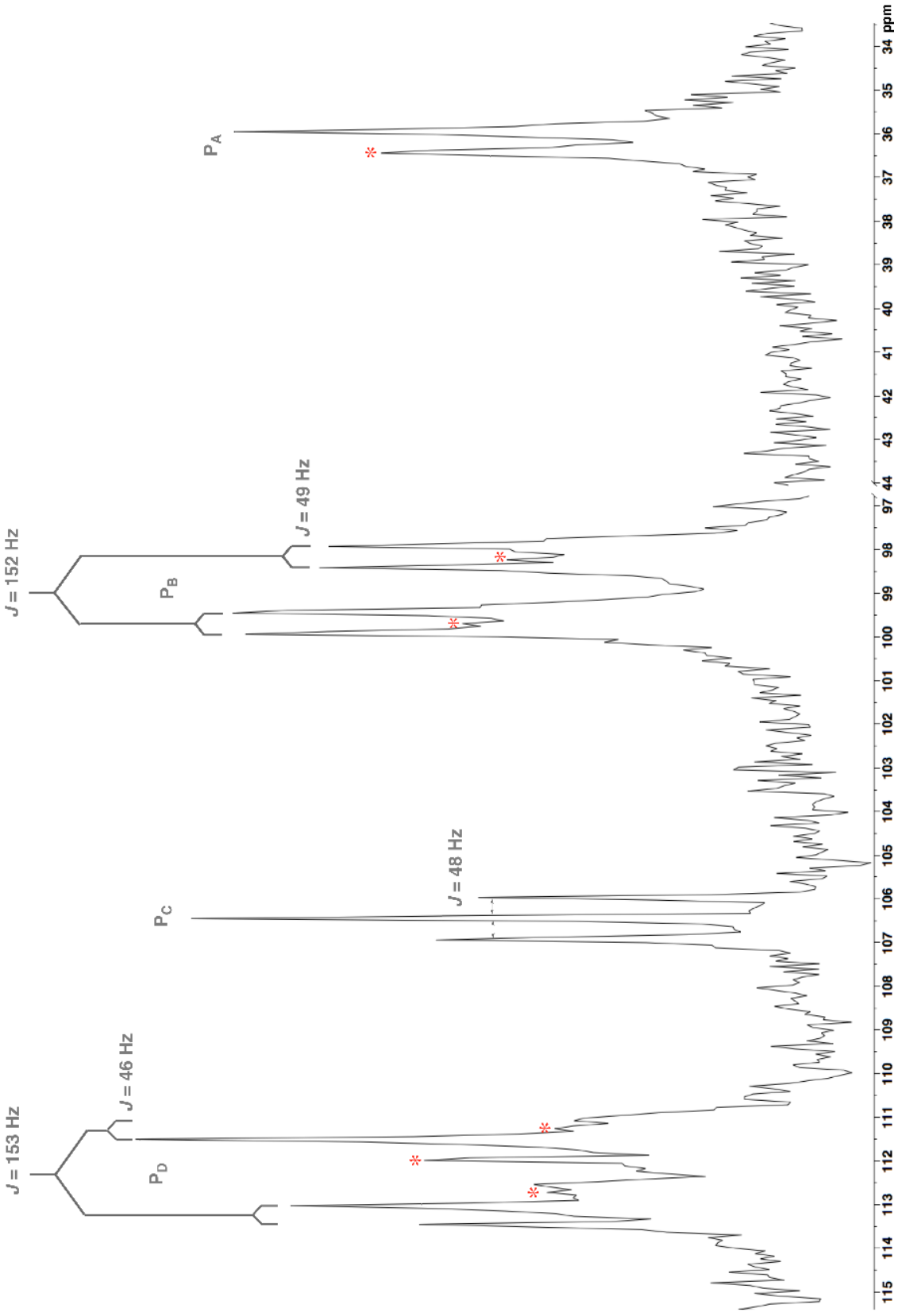

Figure 6.12: $^{31}P\{^{1}H\}$ NMR spectrum of $[Fe(PNP^{Clpym}\text{-}Ph)_2Cl]BF_4$

6.6 Fe(PNP-Ph)(CO)Cl_2 Complexes

Synthesis

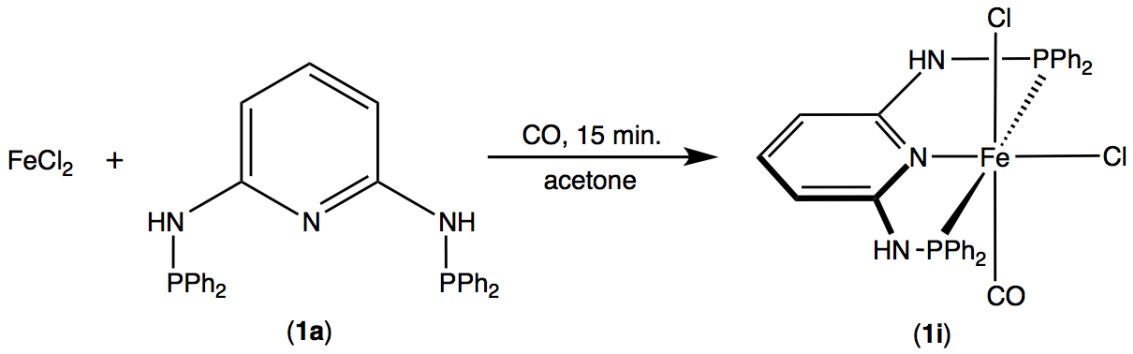

Figure 6.13: Synthesis of Fe(PNP-Ph)(CO)Cl_2 complexes

The Fe(PNP-Ph)(CO)Cl_2 complex **1i** was synthesized by reacting anhydrous $FeCl_2$ with one equiv of the PNP-Ph ligand (**1a**) in acetone or THF under CO atmosphere. Thereby the color of the solution turned red. After a reaction time of about 15 minutes the solvent was removed under reduced pressure to give the product as red solids in high yields (89-90%).

When the reaction was tried with the pyrimidine based ligands, only mixtures of the *cis*- and *trans*-complexes and to some part also the κ^3-κ^2-complexes (see chapter 6.5) could be obtained. Therefore no adequate spectra could obtained for analysis.

Characterization

The complex **1i** was characterized by ^{1}H, ^{31}P{^{1}H} and ^{13}C{^{1}H} NMR spectroscopy. In comparison to the complexes with the *i*Pr ligands, the shifting of the ^{31}P signals compared to the free ligands to lower fields is higher (110.2 ppm for the complex and 37.8 ppm for the free PNP-Ph ligand). It is actually comparable to the shift of the *trans*-species of the *i*Pr complexes.

The other NMR spectra showed signals in the expected areas and ^{13}C showed the CO ligand at 162.3 ppm as triplet.

The molecular structure of *cis*-[Fe(PNP-Ph)(CO)Cl_2] is shown in figure 6.14.

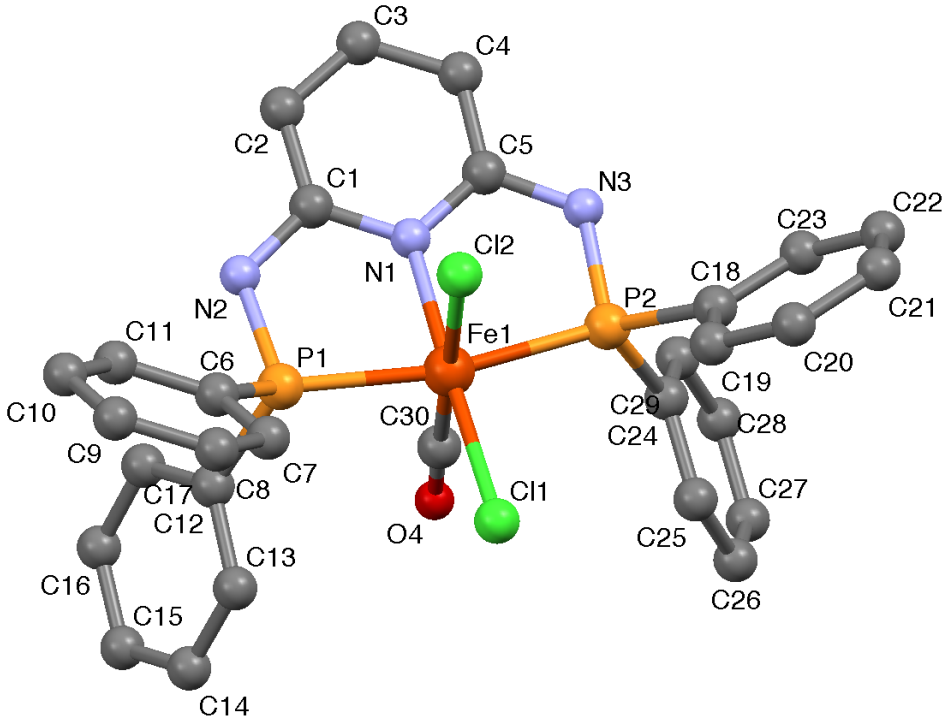

Figure 6.14: ORTEP plot of [Fe(PNP-Ph)(CO)Cl_2] **1i** showing 50% thermal ellipsoids (solvent molecules and H atoms are omitted for clarity)

Selected bond lengths (Å) and angles (deg): Fe(1)-P(1) 2.2248(4), Fe(1)-P(2) 2.2279(4), Fe(1)-N(1) 1.9798(11), Fe(1)-Cl(1) 2.3173(4), Fe(1)-Cl(2) 2.3461(4), P(1)-N(2) 1.6836(13), P(2)-N(3) 1.6907(12), N(1)-C(1) 1.3548(17), N(1)-C(5) 1.3558(16), N(2)-C(1) 1.3700(18), N(3)-C(5) 1.3721(17), P(1)-C(12) 1.8137(15), P(1)-C(6) 1.8172(14), P(2)-C(24) 1.8151(14), P(2)-C(18) 1.8154(14); C(30)-Fe-Cl(2) 177.79(4), P(1)-Fe-P(2) 167.215(15), N(1)-Fe-Cl(1) 176.80(4).

6.7 Synthesis of Hydride Complexes

The first attempt to synthesize the hydride complex **1j** was by reducing the Fe(PNP-*i*Pr)(CO)Cl_2 complex under CO atmosphere to yield the Fe(0) species, which then would be converted to the hydride species with HX (X = Cl^-, BF_4^-). The reaction is shown in figure 6.15.

As reducing agent Zn, Na, Li and sodium naphthalide were used but none of the reactions yielded a clean product. The Fe(0) species could be isolated by treating the product mixture obtained by the reducing step with toluene. After filtering off the remaining solids the red solution treated with ethereal HCl or HBF_4 and the solvent was then removed under vacuum to give the desired hydride species as white solid in very low yields (<3%).

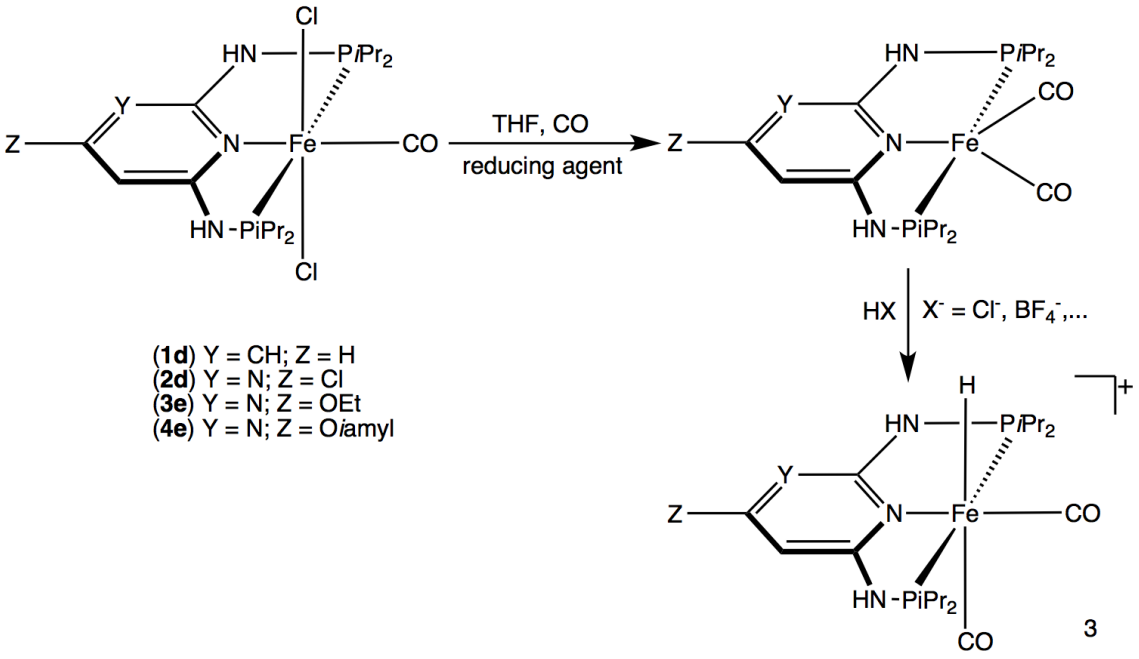

Figure 6.15: Synthesis of hydride complexes via Fe(0)

When the Fe(PNP-*i*Pr)$(CO)_2$Cl complexes were used as starting materials and treated with Zn in THF for 12-24h the hydride species formed immediately. With this reaction much better yields could be obtained, but the product could not be isolated from the unknown byproducts. Conducting the reaction under hydrogen atmosphere reduced the reaction time to a few hours. Figure 6.16 shows the proposed mechanism leading to the hydride complexes. It is suggested that the resulting species is the neutral complex **2** contrary to the reaction in figure 6.15, where the cationic complex **3** is formed.

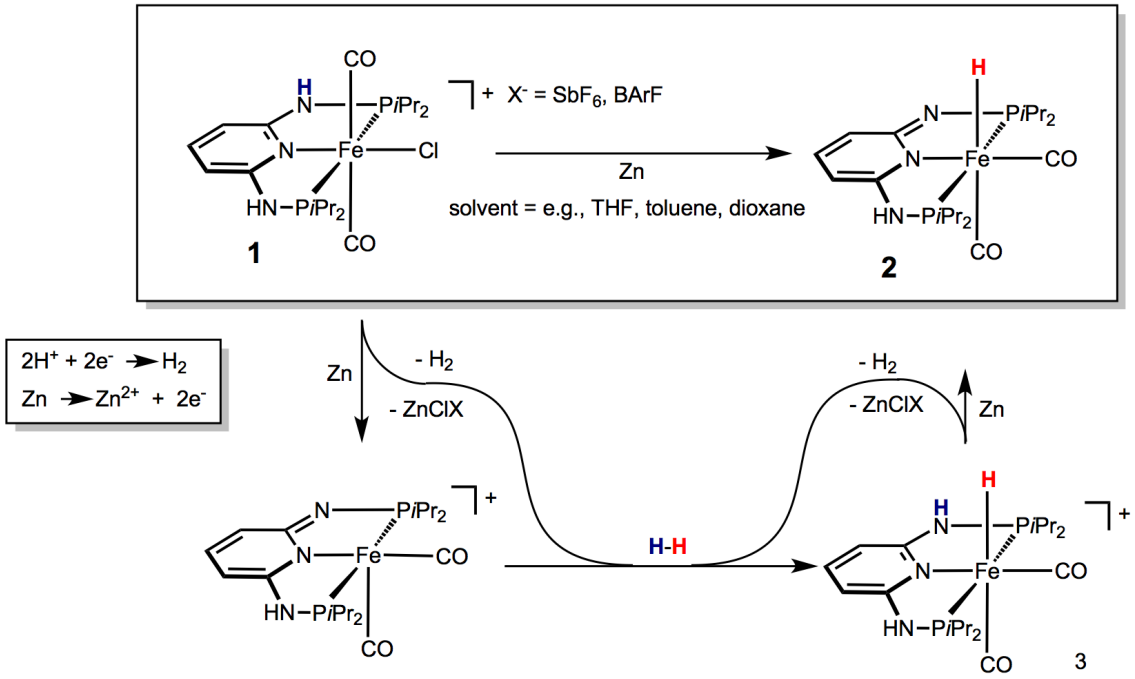

Figure 6.16: Proposed mechanism of hydride formation under reductive conditions

7. CO Binding at Iron Pincer Complexes

The selective and reversible binding of CO to Fe(PNP-*i*Pr)Cl_2 (**1c**) was already described in literature [65]. In the course of this work the complexes Fe(PNP^{Clpym}-*i*Pr)Cl_2 (**2c**) and Fe($PNP^{OIsopym}$-*i*Pr)Cl_2 (**4d**) were analyzed regarding their ability to bind and cede CO. The time dependency of this process was monitored with IR spectroscopy, where the change of the stretching vibration of coordinated CO in **2e** ($\tilde{\nu}_{C=O}$= 1957 cm^{-1}) and **4f** ($\tilde{\nu}_{C=O}$= 1959 cm^{-1}) was determined. Powder samples of the complexes were used and measured in diffuse reflectance. The reaction of **2c** and **4d** with CO was carried out at room temperature with 0.4 bar CO pressure for 5 minutes. The desorption of CO was performed by raising the temperature to 70 °C for **2e** and 50 °C for **4f** respectively within 5 minutes and then holding the temperature for another 25-30 minutes. Figures 7.1 and 7.2 show the time dependency curves obtained.

As can easily be seen comparing the two figures, the addition and desorption of CO is much faster with the Fe($PNP^{OIsopym}$-*i*Pr)Cl_2 (**4d**) complex than with Fe(PNP^{Clpym}-*i*Pr)Cl_2 (**2c**) even at lower temperatures. Compared to Fe(PNP-*i*Pr)Cl_2 (**1c**) described in literature [65] the two systems examined in this work (**2c** and **4d**) show faster desorption at lower temperatures and at higher pressures despite of approximately the same addition rate.

The Fe($PNP^{OIsopym}$-*i*Pr)Cl_2 (**4d**) complex already loses CO when stored at room temperature over night. The loss is about the same as if the complex was heated to 50 °C for 10 minutes.

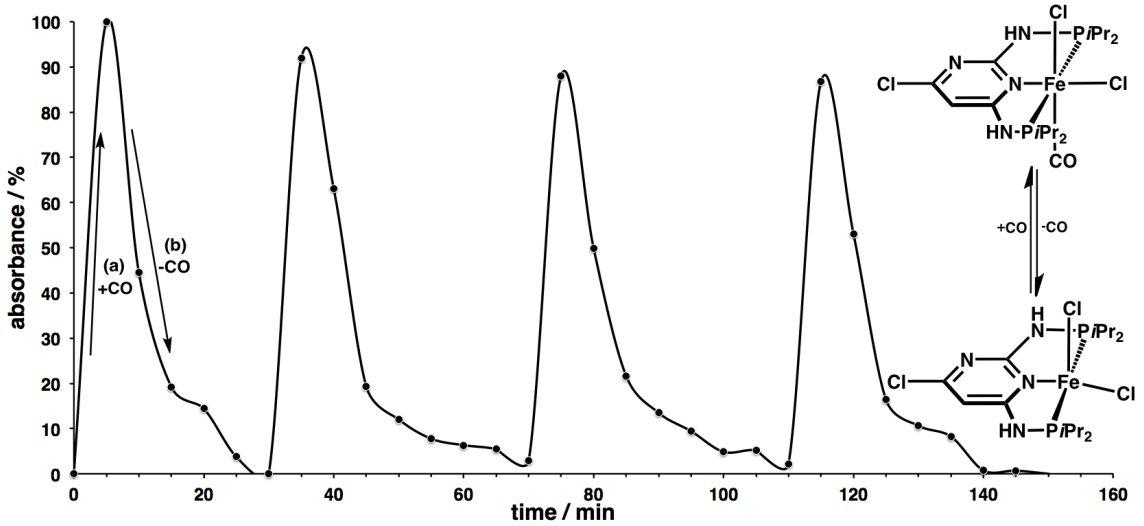

Figure 7.1: Time dependence of the intensity of the stretching frequency $\tilde{\nu}_{C=O}$= 1957 cm^{-1} of **2e**: a) increase during the reaction of **2c** and CO at RT and 0.4 bar CO; b) decrease upon heating to 70 °C at 970 mbar

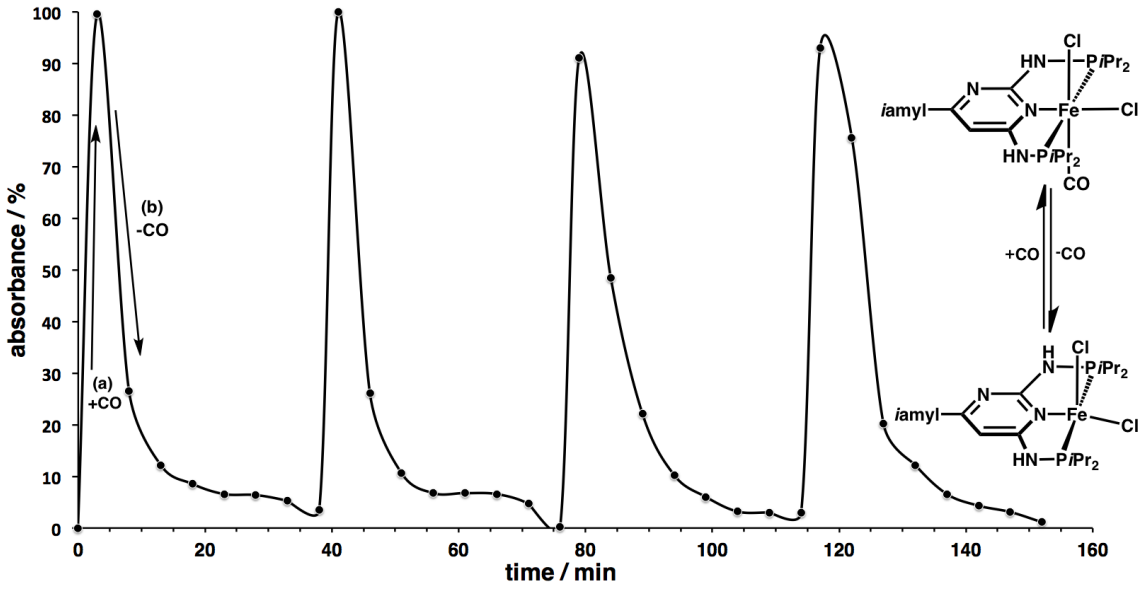

Figure 7.2: Time dependence of the intensity of the stretching frequency $\tilde{\nu}_{C=O}$= 1959 cm^{-1} of **4f**: a) increase during the reaction of **4d** and CO at RT and 0.4 bar CO; b) decrease upon heating to 50 °C at 970 mbar

8. Summary

The PNP ligands used in this work are very easy to prepare and modulate with a wide range of commercially available precursors. All ligand syntheses work with large quantities in excellent yields. With this synthesis route even chiral phosphines can be introduced easily.

The paramagnetic Fe(PNP-*i*Pr)Cl_2 are prepared easily and give air and moisture stable complexes in very good yields with all PNP-*i*Pr ligands prepared in this work.

The mono-CO complexes Fe(PNP-*i*Pr)Cl_2CO can be prepared as *cis*- and *trans*-complexes in excellent yields. The stability of the *cis*-complexes depends largely on which ligands were used. The pyridine based complex is the most stable one and loses CO very slowly, whereas the pyrimidine based ligands lose CO much faster when stored under air.

The synthesis of Fe(PNP-*i*Pr)ClCO_2 complexes was also very simple and resulted in relatively air and moisture stable compounds in good yields.

Reactions conducted with the PNP-Ph ligands gave unexpected [Fe(PNP-Ph)$_2$Cl]$^+$ complexes and the mono-CO complexes could be obtained when the reaction was carried out under CO atmosphere.

Syntheses of hydride complexes did not give enough product or did not yield in clean compounds so no catalytical studies could be done.

CO addition and desorption studies were carried out with Fe(PNP^{OIsopym}-*i*Pr)Cl_2 and Fe(PNP^{Clpym}-*i*Pr)Cl_2, which showed that these complexes can easily emit the CO ligand and therefore would be nice chromogenic gas sensors.

Part III

EXPERIMENTAL PART

9. General

All reactions, unless stated differently, were performed under inert atmosphere using Schlenk techniques or inside a glove box. Solvents were dried and purified according to standard procedures [67]. Deuterated solvents were purchased from Aldrich and Eurisotop, degassed using freeze-pump-thaw technique and stored over 4 $\mathring{A}$ molecular sieves. ^{1}H, $^{13}C\{^{1}H\}$ and $^{31}P\{^{1}H\}$ NMR spectra were recorded on a Bruker AVANCE-250 spectrometer operating at 250.13 (^{1}H), 62.86 (^{13}C) and 101.26 (^{31}P) MHz and were referenced to $SiMe_4$ and H_3PO_4 (85%), respectively.

10. Organic Precursors

10.1 Diaminopyrimidines

2,6-Diamino-4-ethoxypyrimidine [60] (3a)

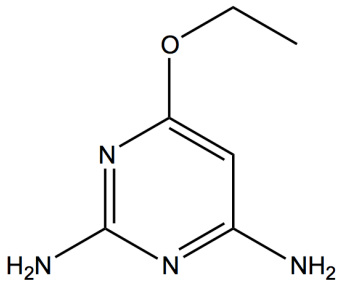

To a solution of NaH (2.32 g, 97 mmol) in ethanol (100 mL) 2,6-diamino-4-chloropyrimidine (7 g, 48 mmol) was added. The mixture was refluxed for 12 h. After cooling the solvents were removed under vacuum and the remaining oil was purified by flash chromatography on silica gel (CH_2Cl_2/MeOH 4:1) to give **3a** as a white solid.

Yield: 5.79 g (78%) white solid; $C_6H_{10}N_4O$ (MW: 154.17); 46.74% C, 6.54% H, 36.34% N, 10.38% O.
^{1}H NMR (δ, DMSO-d_6, 20 °C): 5.98 (bs, 2H, NH_2), 5.81 (bs, 2H, NH_2), 5.00 (s, 1H, pym5), 4.09 (q, J = 7.0 Hz, 2H, OCH_2CH$_3$), 1.19 (t, J = 6.9 Hz, 3H, OCH$_2$CH_3).
^{13}C{^{1}H} NMR (δ, DMSO-d_6, 20 °C): 170.4 (pym^4), 166.4 (pym^6), 163.4 (pym^2), 76.5 (pym^5), 60.7 (OCH$_2$CH$_3$), 15.1 (OCH$_2$$CH_3$).

2,6-Diamino-4-isoamyloxypyrimidine (4a)

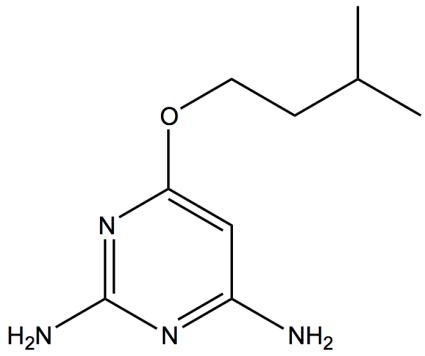

This compound was prepared analogously to **3a** using NaH (2.32 g, 97 mmol), isoamyl alcohol (100 mL) and 2,6-diamino-4-chloropyrimidine (7 g, 48 mmol) as starting materials.

Yield: 8.13 g (86%) white solid; $C_9H_{16}N_4O$ (MW: 196.25); 55.08% C, 8.22% H, 28.55% N, 8.15% O.

^{1}H NMR (δ, DMSO-d_6, 20 °C): 5.95 (bs, 2H, NH_2), 5.80 (bs, 2H, NH_2), 5.00 (s, 1H, pym5), 4.08 (t, J = 6.6 Hz, 2H, OCH_2CH$_2$CH(CH$_3$)$_2$), 1.66 (sept, J = 6.6 Hz, 1H, OCH$_2$CH$_2$CH(CH$_3$)$_2$), 1.48 (q, J = 6.7 Hz, 2H, OCH$_2$CH_2CH(CH$_3$)$_2$), 0.88 (d, J = 6.5 Hz, 6H, OCH$_2$CH$_2$CH(CH_3)$_2$).

^{13}C{^{1}H} NMR (δ, DMSO-d_6, 20 °C): 170.6 (pym^4), 166.4 (pym^6), 163.4 (pym^2), 76.5 (pym^5), 63.4 (OCH$_2$CH$_2$CH(CH$_3$)$_2$), 37.9 (OCH$_2$$CH_2$CH(CH$_3$)$_2$), 25.0 (OCH$_2CH_2$$C$H(CH$_3$)$_2$), 22.9 (OCH$_2CH_2$CH($CH_3$)$_2$).

11. Ligands

N,N'-Bis(diphenylphosphino)-2,6-diaminopyridine (PNP-Ph) [63] (1a)

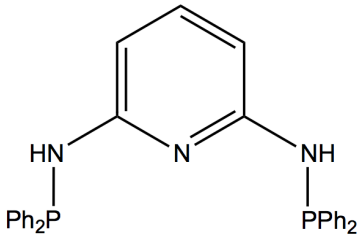

Triethylamine (10.0 mL, 73 mmol) was added to a suspension of 2,6-diaminopyridine (4.0 g, 37 mmol) in toluene (120 mL). The mixture was cooled to 0 °C and PPh_2Cl (13 mL, 73 mmol) was added dropwise. The reaction mixture was heated to 80 °C and was stirred at that temperature overnight. The solution was then filtered and the solvent was removed under reduced pressure to give 1a as a white solid. If necessary (NMR) the obtained solid was recrystallized from toluene/n-hexane (1:1).

Yield: 14.3 g (81%) white solid; $C_{29}H_{25}N_3P_2$ (MW: 477,48); 72.95% C, 5.28% H, 8.80% N, 12.97% P.

^{1}H NMR (δ, $CDCl_3$, 20 °C): 7.46-7.34 (m, 21H, Ph, py^4), 6.50 (dd, J = 7.9 Hz, J = 1.6 Hz, 2H, py^{3,5}), 5.04 (s, 2H, NH).

^{13}C{^{1}H} NMR (δ, $CDCl_3$, 20 °C): 157.6 (d, J = 20.2 Hz, py^{2,6}), 139.9 (d, J = 12.1 Hz, py^4), 134.0 (Ph^1), 131.3 (d, J = 20.9 Hz, Ph^{2,6}), 129.2 (Ph^4), 128.58 (d, J = 6.7 Hz, Ph^{3,5}), 99.2 (d, J = 14.8 Hz, py^{3,5}).

^{31}P{^{1}H} NMR (δ, $CDCl_3$, 20 °C): 37.8.

N,N'-Bis(diisopropylphosphino)-2,6-diaminopyridine (PNP-^{i}Pr) [63] (1b)

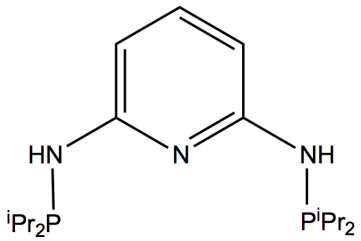

This ligand was prepared analogously to **1a** with NEt_3 (9.7 mL, 70 mmol), 2,6-diaminopyridine (3.82 g, 35 mmol) and PiPr$_2$Cl (11.6 mL, 70 mmol) as starting materials.

Yield: 9.6 g (80%) white solid; $C_{17}H_{33}N_3P_2$ (MW: 341.41); 59.81% C, 9.74% H, 12.31% N, 18.14 % P.

^{1}H NMR (δ, $CDCl_3$, 20 °C): 7.26 (t, J = 8.0 Hz, 1H, py^4), 6.44 (dd, J = 8.0 Hz, J = 2.1 Hz, 2H, py^{3,5}), 4.49 (d, J = 8.9 Hz, 2H, NH), 1.80-1.66 (m, 4H, CH(CH_3)$_2$), 1.09-0.99 (m, 24H, CH(CH_3)$_2$)

^{13}C{^{1}H} NMR (δ, $CDCl_3$, 20 °C): 159.5 (d, J = 20.3 Hz, py^{2,6}), 139.1 (py^4), 98.1 (d, J = 18.4 Hz, py^{3,5}), 26.3 (d, J = 10.7 Hz, CH(CH$_3$)$_2$), 18.6 (d, J = 19.6 Hz , CH(CH$_3$)$_2$), 17.2 (d, J = 7.7 Hz, CH(CH$_3$)$_2$).

^{31}P{^{1}H} NMR (δ, $CDCl_3$, 20 °C): 60.4.

N,N'-Bis(diphenylphosphino)-2,6-diamino-4-chloropyrimidine (PNP^{ClPym}-Ph) (2a)

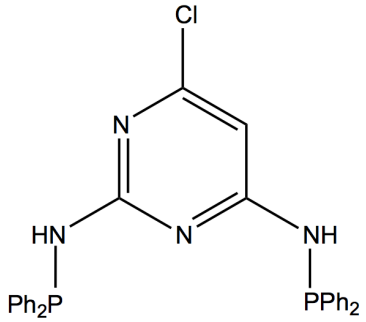

This ligand was prepared analogously to **1a** with NEt_3 (9.6 mL, 69 mmol), 2,6-diamino-4-chloropyrimidine (5 g, 35 mmol) and PPh_2Cl (12.8 mL, 69 mmol) as starting materials.

Yield: 9.78 g (55%); $C_{28}H_{23}ClN_4P_2$ (MW: 512.91); 65.57% C, 4.52% H, 6.91% Cl, 10.92% N, 12.08 % P.

^{1}H NMR (δ, $CDCl_3$, 20 °C): 7.36-7.18 (m, 20H, Ph), 6.49 (d, J = 1.25 Hz, 1H, pym^{5}), 5.46 (d, J = 8.9 Hz, 1H, NH), 5.40 (d, J = 8.8 Hz, 1H, NH).
^{13}C{^{1}H} NMR (δ, $CDCl_3$, 20 °C): 165.8 (d, J = 21.3 Hz, pym^{6}), 162.4 (d, J = 19.5 Hz, pym^{2}), 160.7 (s, pym^{4}), 139.1 (d, J = 13.4 Hz, Ph^{1}), 137.7 (d, J = 10.6 Hz, Ph$^{1'}$), 131.6 (d, J = 5.7 Hz, Ph^{2,6}), 131.3 (d, J = 5.9 Hz, Ph$^{2',6'}$), 129.8 (s, Ph^{4}), 129.4 (s, Ph$^{4'}$), 128.8 (d, J = 6.9 Hz, Ph^{3,5}), 128.6 (d, J = 6.7 Hz, Ph$^{3',5'}$), 95.9 (d, J = 18.9 Hz, pym^{5}).
^{31}P{^{1}H} NMR (δ, $CDCl_3$, 20 °C): 39.6, 37.6.

N,N'-Bis(diisopropylphosphino)-2,6-diamino-4-chloropyrimidine (PNP^{ClPym}-^{i}Pr) [64] (2b)

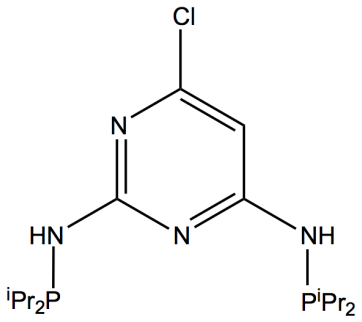

This ligand was prepared analogously to **1a** with NEt_3 (3.8 mL, 28 mmol), 2,6-diamino-4-chloropyrimidine (2.0 g, 14 mmol) and PiPr$_2$Cl (4.6 mL, 28 mmol) as starting materials.

Yield: 4.44 g (85%) white solid; $C_{16}H_{31}ClN_4P_2$ (MW: 376.84); 50.99% C, 8.29% H, 9.41% Cl, 14.87% N, 16.44 % P.
^{1}H NMR (δ, $CDCl_3$, 20 °C): 6.51 (d, J = 2.25 Hz, 1H, pym^{5}), 5.04-4.86 (m, 2H, NH), 1.80-1.72 (m, 4H, CH(CH$_3$)$_2$), 1.06-0.99 (m, 24H, CH(CH_3)$_2$).
^{13}C{^{1}H} NMR (δ, $CDCl_3$, 20 °C): 167.7 (d, J = 21.3 Hz, pym^{6}), 163.8 (d, J = 13.8 Hz, pym^{4}), 159.8 (s, pym^{2}), 95.4 (d, J = 20.7 Hz, pym^{5}), 26.1 (d, J = 10.3 Hz, CH(CH$_3$)$_2$), 26.0 (d, J = 11.0 Hz, CH(CH$_3$)$_2$), 18.5 (d, J = 19.5 Hz, CH(CH$_3$)$_2$), 18.4 (d, J = 19.5 Hz, CH(CH$_3$)$_2$), 17.2 (vt, J = 8.6 Hz, CH(CH$_3$)$_2$).
^{31}P{^{1}H} NMR (δ, $CDCl_3$, 20 °C): 62.9, 60.3.

N,N'-Bis(diphenylphosphino)-2,6-diamino-4-ethoxypyrimidine (PNP^{OEtPym}-Ph) (3b)

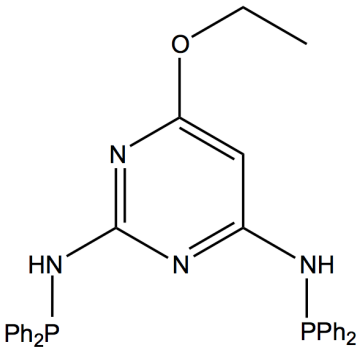

This ligand was prepared analogously to **1a** with NEt_3 (3.6 mL, 26 mmol), 2,6-diamino-4-ethoxypyrimidine (**3a**) (2 g, 13 mmol) and PPh_2Cl (4.7 mL,26 mmol) as starting materials.

Yield: 6.54 g (96%) white solid; $C_{30}H_{28}N_4OP_2$ (MW: 522.52); 68.96% C, 5.40% H, 10.72% N, 3.06% O, 11.86 % P.

^{1}**H NMR** (δ, $CDCl_3$, 20 °C): 7.43-7.19 (m, 20H, Ph), 5.89 (d, J = 1.60 Hz, 1H, pym^5), 5.27 (s, 1H, NH), 5.23 (s, 1H, NH), 4.22 (q, J = 7.08 Hz, 2H, OCH_2CH$_3$), 1.27 (t, J = 7.04 Hz, 3H, OCH$_2$CH_3).

^{13}**C{^{1}H} NMR** (δ, $CDCl_3$, 20 °C): 171.2 (s, pym^4), 166.1 (d, J = 24.5 Hz, pym^6), 162.2 (d, J = 16.2 Hz, pym^2), 139.8 (d, J = 14.5 Hz, Ph^1), 138.7 (d, J = 11.4 Hz, Ph$^{1'}$), 131.6 (d, J = 3.5 Hz, Ph^{2,6}), 131.3 (d, J = 3.2 Hz, Ph$^{2',6'}$), 129.4 (s, Ph^4), 129.1 (s, Ph$^{4'}$), 128.6 (d, J = 6.8 Hz, Ph^{3,5}), 128.4 (d, J = 6.7 Hz, Ph$^{3',5'}$), 80.2 (d, J = 18.2 Hz, pym^5), 62.0 (s, OCH$_2$CH$_3$), 14.5 (s, OCH$_2$$CH_3$).

^{31}**P{^{1}H} NMR** (δ, $CDCl_3$, 20 °C): 37.9, 37.6.

N,N'-Bis(diisopropylphosphino)-2,6-diamino-4-ethoxypyrimidine (PNP^{OEtPym}-^{i}Pr) [64] (3c)

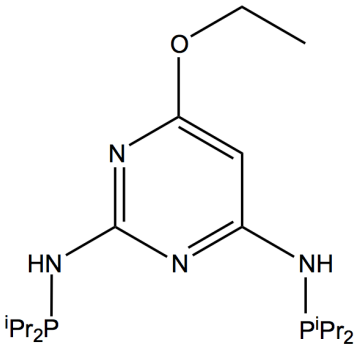

This ligand was prepared analogously to **1a** with NEt_3 (9 mL, 65 mmol), 2,6-diamino-4-ethoxypyrimidine (**3a**) (5 g, 32 mmol) and P*i*Pr_2Cl (15.5 mL, 65 mmol) as starting materials.

Yield: 10.46 g (83%) white solid; $C_{18}H_{36}N_4OP_2$ (MW: 386.45); 55.94% C, 9.39% H, 14.50% N, 4.14 % O, 16.03 % P.

^{1}H NMR (δ, $CDCl_3$, 20 °C): 5.85 (d, J = 2.2 Hz, 1H, pym^{5}), 4.72 (vt, J = 9.6 Hz, 2H, N*H*), 4.25 (q, J = 7.0 Hz, 2H, OC$H_2$$CH_3$), 1.85-1.69 (m, 4H, C*H*$(CH_3)_2$), 1.34 (t, J = 7.0 Hz, OCH_2CH_3), 1.12-0.99 (m, 24H, $CH(CH_3)_2$).

^{13}C{^{1}H} NMR (δ, $CDCl_3$, 20 °C): 170.8 (s, pym^{4}), 167.7 (dd, J = 2.7 Hz, J = 20.3 Hz, pym^{6}), 163.5 (dd, J = 2.3 Hz, J = 11.9 Hz, pym^{2}), 79.0 (s, pym^{5}), 62.0 (s, CH_2), 26.2 (d, J = 13.1 Hz, *C*$H(CH_3)_2$), 26.1 (d, J = 11.5 Hz, *C*$H(CH_3)_2$), 18.7 (d, J = 15.0 Hz, $CH(CH_3)_2$), 18.5 (d, J = 14.6 Hz, $CH(CH_3)_2$), 17.4 (d, J = 8.8 Hz, $CH(CH_3)_2$), 17.1 (d, J = 8.0 Hz, $CH(CH_3)_2$), 14.6 (s, *C*H_3).

^{31}P{^{1}H} NMR (δ, $CDCl_3$, 20 °C): 61.6, 60.5.

N,N'-Bis(diphenylphosphino)-2,6-diamino-4-isoamyloxypyrimidine ($PNP^{OIsoPym}$-Ph) (4b)

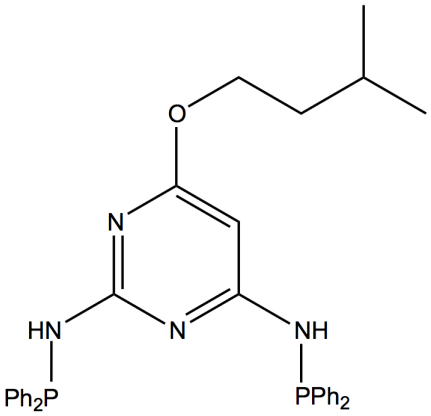

This ligand was prepared analogously to **1a** with NEt_3 (8.1 mL, 58 mmol), 2,6-diamino-4-isoamyloxypyrimidine (**4a**) (5.7 g, 29 mmol) and PPh_2Cl (9.5 mL, 58 mmol) as starting materials.

Yield: 12.30 g (75%) yellow solid; $C_{33}H_{34}N_4OP_2$ (MW: 564.60); 70.20% C, 6.07% H, 9.92% N, 2.83% O, 10.97 % P.

^{1}H NMR (δ, $CDCl_3$, 20 °C): 7.45-7.34 (m, 20H, Ph), 5.89 (d, J = 1.3 Hz, 1H, pym^5), 5.27 (s, 1H, NH), 5.23 (s, 1H, NH), 4.19 (t, J = 6.7 Hz, 2H, OCH_2CH$_2$CH(CH$_3$)$_2$)) , 1.79-1.49 (m, 3H, OCH$_2$CH_2CH(CH$_3$)$_2$), 0.95-0.87 (m, 6H, (CH_3)$_2$).

^{13}C{^{1}H} NMR (δ, $CDCl_3$, 20 °C): 171.3 (s, pym^4), 166.1 (d, J = 22.5 Hz, pym^6), 162.1 (d, J = 16.5 Hz, pym^2), 139.8 (d, J = 14.3 Hz, Ph^1), 138.7 (d, J = 11.0 Hz, Ph$^{1'}$), 131.6 (d, J = 4.1 Hz, Ph^{2,6}), 131.3 (d, J = 3.7 Hz, Ph$^{2',6'}$), 129.4 (s, Ph^4), 129.1 (s, Ph$^{4'}$), 128.6 (d, J = 6.7 Hz, Ph^{3,5}), 128.4 (d, J = 6.5 Hz, Ph3′, 5′), 80.1 (d, J = 18.4 Hz, pym^5), 64.7 (s, OCH$_2$CH$_2$CH(CH$_3$)$_2$), 37.7 (s, OCH$_2$$CH_2$CH(CH$_3$)$_2$), 24.9 (s, OCH$_2CH_2$$C$H(CH$_3$)$_2$), 22.5 (s, OCH$_2CH_2$CH($CH_3$)$_2$).

^{31}P{^{1}H} NMR (δ, $CDCl_3$, 20 °C): 37.9, 37.33.

N,N'-Bis(diisopropylphosphino)-2,6-diamino-4-isoamyloxypyrimidine ($PNP^{OIsoPym}$-^{i}Pr) (4c)

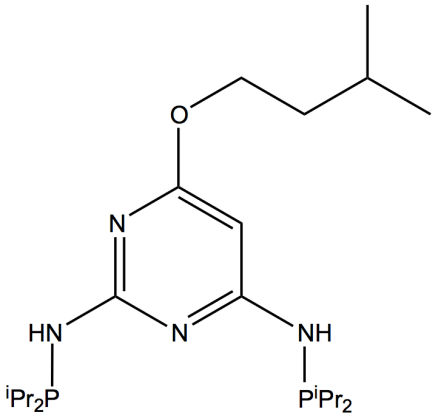

This ligand was prepared analogously to **1a** with NEt_3 (7.1 mL, 51 mmol), 2,6-diamino-4-isoamyloxypyrimidine (**4a**) (5 g, 25 mmol) and P*i*Pr_2Cl (8.5 mL, 51 mmol) as starting materials.

Yield: 6.31 g (58%) yellow solid; $C_{21}H_{42}N_4OP_2$ (MW: 428.53); 58.86% C, 9.88% H, 13.07% N, 3.73% O, 14.46 % P.

^{1}H NMR (δ, $CDCl_3$, 20 °C): 5.83 (d, J = 2.2 Hz, 1H, pym^5), 4.74 (vt, J = 8.6 Hz, 2H, N*H*), 4.19 (t, J = 6.7 Hz, 2H, OC*H*$_2$CH$_2$CH(CH$_3$)$_2$), 1.84-1.69 (m, 4H, C*H*(CH$_3$)$_2$), 1.58 (q, J = 7.0 Hz, OCH$_2$C*H*$_2$CH(CH$_3$)$_2$), 1.28-1.17 (m, 1H, OCH$_2$CH$_2$C*H*(CH$_3$)$_2$), 1.11-0.90 (m, 24H, CH(C*H*$_3$)$_2$).

^{13}C{^{1}H} NMR (δ, $CDCl_3$, 20 °C): 171.0 (s, pym^4), 167.7 (d, J = 20.4 Hz, pym^6), 163.4 (d, J = 14.2 Hz, pym^2), 79.2 (d, J = 20.2 Hz, pym^5), 64.7 (s, O*C*H$_2$CH$_2$CH(CH$_3$)$_2$), 37.8 (s, OCH$_2$*C*H$_2$CH(CH$_3$)$_2$), 26.3 (d, J = 6.4 Hz, *C*H(CH$_3$)$_2$), 26.1 (d, J = 4.4 Hz, *C*H(CH$_3$)$_2$), 24.9 (s, OCH$_2$CH$_2$*C*H(CH$_3$)$_2$), 22.6 (s, OCH$_2$CH$_2$CH(*C*H$_3$)$_2$), 18.8 (d, J = 14.7 Hz, CH(*C*H$_3$)$_2$), 18.5 (d, J = 14.0 Hz, CH(*C*H$_3$)$_2$), 17.5 (d, J = 8.7 Hz, CH(*C*H$_3$)$_2$), 17.1 (d, J = 7.9 Hz, CH(*C*H$_3$)$_2$), 14.6 (s, *C*H$_3$).

^{31}P{^{1}H} NMR (δ, $CDCl_3$, 20 °C): 60.1.

12. Complexes

12.1 PNP-iPr Complexes

Fe(PNP-iPr)Cl_2 [63] (1c)

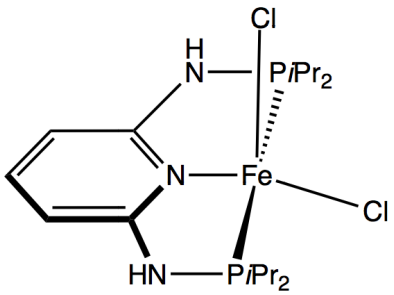

To a suspension of $FeCl_2$ (185 mg, 1.46 mmol) in acetone PNP-*i*Pr (500 mg, 1.46 mmol) was added. The reaction mixture was stirred overnight at room temperature. The solvent was then removed under reduced pressure and the remaining yellow solid was washed thrice with Et_2O (10 mL) and dried under vacuum.

Yield: 625 mg (94%) yellow solid; $C_{17}H_{33}Cl_2FeN_3P_2$ (MW: 468.16); 43.61% C, 7.10% H, 15.15% Cl, 11.99% Fe, 8.98% N, 13.23% P.
^{1}H NMR (δ, acetone-d_6, 20 °C, all peaks appear as broad singlets): 140.00 (CH(CH_3)$_2$), 72.89 (NH), 47.52 (py^{3,5}), 12.98 (CH(CH_3)$_2$), 6.84 (CH(CH_3)$_2$), -21.10 (py^4).

trans-[Fe(PNP-iPr)(CO)Cl_2] [65] (1d)

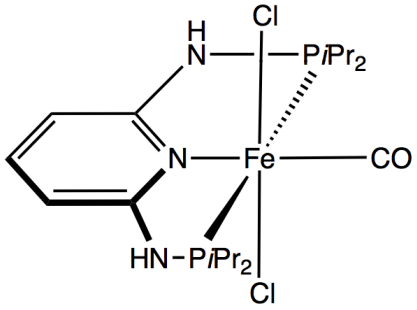

CO was bubbled into a solution of **1c** (625 g, 1.34 mmol) in acetone for 5 minutes, whereupon the color of the reaction mixture turned from yellow to blue. The solvent was then removed under reduced pressure and the remaining solid was dried under vacuum.

Yield: 629 mg (95%) blue solid; $C_{18}H_{33}Cl_2FeN_3OP_2$ (MW: 496.17); 43.57% C, 6.70% H, 14.29% Cl, 11.26% Fe, 8.47% N, 3.22%O, 12.49% P.

^{1}H NMR (δ, DMSO-d_6, 20 °C): 8.50 (s, 2H, NH), 7.42 (t, J = 7.3 Hz, 1H, py^4), 6.47 (d, J = 7.2 Hz, 2H, py^{3,5}), 2.76 (m, 4H, CH(CH$_3$)$_2$), 1.43-1.27 (m, 24H, CH(CH_3)$_2$).

^{13}C{^{1}H} NMR (δ, DMSO-d_6, 20 °C): 224.81 (t, J = 22.7 Hz, CO), 163.1 (t, J = 9.2 Hz, py^{2,6}), 139.8 (py^4), 98.7 (py^{3,5}), 25.5 (t, J = 11.8 Hz, CH(CH$_3$)$_2$), 19.3 (CH(CH$_3$)$_2$), 18.1 (CH(CH$_3$)$_2$).

^{31}P{^{1}H} NMR (δ, DMSO-d_6, 20 °C): 133.1.

IR (ATR, cm^{-1}): 1956 ($\nu_{C=O}$).

cis-[Fe(PNP-iPr)(CO)Cl_2] [65] (1e)

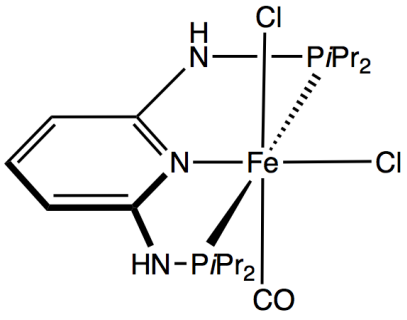

CO was passed over a sample of **1c** (625 mg, 1.34 mmol) in acetone for 5 minutes, whereupon the color of the solid turned from yellow to red.

Yield: 662 mg (100%) red solid; $C_{18}H_{33}Cl_2FeN_3OP_2$ (MW: 496.17); 43.57% C, 6.70% H, 14.29% Cl, 11.26% Fe, 8.47% N, 3.22%O, 12.49% P.
^{1}H NMR (δ, DMSO-d_6, 20 °C): 8.20 (s, 2H, NH), 7.06 (t, J = 6.7 Hz, 1H, py^4), 6.01 (d, J = 6.8 Hz, 2H, py^{3,5}), 2.48 (m, 4H, CH(CH$_3$)$_2$), 1.42-1.27 (m, 24H, CH(CH_3)$_2$).
^{31}P{^{1}H} NMR (δ, DMSO-d_6, 20 °C): 117.3.
IR (ATR, cm^{-1}): 1947 ($\nu_{C=O}$).

trans-[Fe(PNP-iPr)(CO)$_2$Cl]SbF$_6$ [66] (1f)

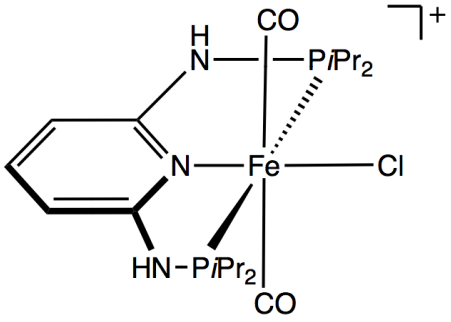

To a solution of **1d** (500 mg, 1.08 mmol) in acetone $AgSbF_6$ (346 mg, 1.08 mmol) was added and CO was bubbled into the reaction mixture for 5 minutes. The reaction mixture was stirred for 30 minutes. Then the precipitate of AgCl was filtered off and the remaining solvent was then removed under reduced pressure. The red solid was washed thrice with Et_2O (10 mL) and dried under vacuum.

Yield: 686 mg (94%) red solid; $C_{19}H_{33}ClF_6FeN_3O_2P_2Sb$ (MW: 724.48); 31.50% C, 4.59% H, 4.89% Cl, 15.73% F, 7.71% Fe, 5.80% N, 4.42%O, 8.55% P, 16.81% Sb.
^{1}H NMR (δ, CD_3NO_2, 20 °C): 7.29 (t, J = 7.8 Hz, 1H, py^4), 6.63 (s, 2H, NH), 6.21 (d, J = 7.8 Hz, 2H, py^{3,5}), 3.25 (m, 4H, CH(CH$_3$)$_2$), 1.56 (d, J = 7.5 Hz, 24H, CH(CH$_3$)$_2$).
^{13}C{^{1}H} NMR (δ, CD_3NO_2, 20 °C): 211.6 (t, J = 24.4 Hz, CO), 161.4 (t, J = 6.2 Hz, py^{2,6}), 141.2 (py^4), 100.0 (t, J = 3.0 Hz, py^{3,5}), 31.7 (vt, J = 12.2 Hz, CH(CH$_3$)$_2$), 16.9 (d, J = 3.7 Hz CH(CH$_3$)$_2$).
^{31}P{^{1}H} NMR (δ, CD_3NO_2, 20 °C): 129.7.
IR (ATR, cm^{-1}): 2015 ($\nu_{C=O}$).

Fe(PNP^{Clpym}-iPr)Cl$_2$ [64] (2c)

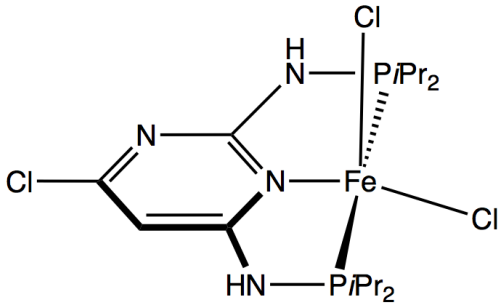

This complex was prepared analogously to **1c** with $FeCl_2$ (680 mg, 5.37 mmol) and PNP-*i*Pr (2.02 g, 5.37 mmol) as starting materials.

Yield: 2.65 g (98%) yellow solid; $C_{16}H_{31}Cl_3FeN_4P_2$ (MW: 503.60); 38.16% C, 6.20% H, 21.12% Cl, 11.09% Fe, 11.13% N, 12.30% P.
^{1}H NMR (δ, acetone-d_6, 20 °C): 139.61 (s, 2H, C*H*(CH$_3$)$_2$), 138.92 (s, 2H, C*H*(CH$_3$)$_2$), 75.61 (s, 1H, N*H*), 75.27 (s, 1H, N*H*), 35.17 (s, 1H, pym^5), 12.41 (s, 6H, CH(C*H*$_3$)$_2$), 11.59 (s, 6H, CH(C*H*$_3$)$_2$), 7.12 (s, 6H, CH(C*H*$_3$)$_2$), 6.66 (s, 6H, CH(C*H*$_3$)$_2$).

***trans*-[Fe(PNP^{Clpym}-iPr)(CO)Cl$_2$] [64] (2d)**

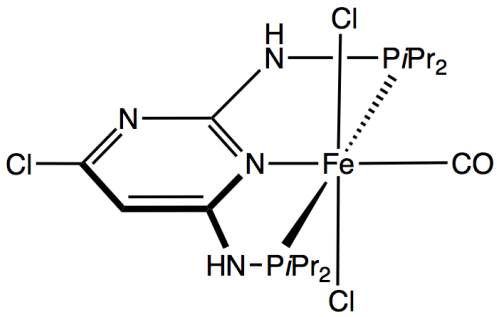

This complex was prepared analogously to **1d** with **2c** (2.65 g, 5.21 mmol) as starting material.

Yield: 2.77 g (99%) violet solid; $C_{17}H_{31}Cl_3FeN_4OP_2$ (MW: 531.61); 38.41% C, 5.88% H, 20.01% Cl, 10.50% Fe, 10.54% N, 3.01%O, 11.65% P.
^{1}H NMR (δ, DMSO-d_6, 20 °C): 9.75 (s, 1H, N*H*), 9.63 (s, 1H, N*H*), 6.69 (s, 1H, pym^5), 2.74 (s, 4H, C*H*(CH$_3$)$_2$), 1.38-1.02 (m, 24 H, CH(C*H*$_3$)$_2$).
^{31}P{^{1}H} NMR (δ, DMSO-d_6, 20 °C): 142.5 (d, J = 177), 128.0 (d, J = 177).
IR (ATR, cm^{-1}): 1972 ($\nu_{C=O}$).

cis-[Fe(PNP^{Clpym}-iPr)(CO)Cl$_2$] [64] (2e)

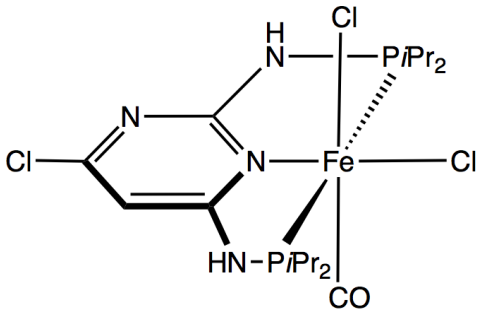

This complex was prepared analogously to **1e** with **2c** (500 mg, 0.99 mmol) as starting material.

Yield: 528 mg (100%) red solid; $C_{17}H_{31}Cl_3FeON_4P_2$ (MW: 531.61); 38.41% C, 5.88% H, 20.01% Cl, 10.50% Fe, 10.54% N, 3.01%O, 11.65% P.
^{31}P{^{1}H} NMR (δ, DMSO-d_6, 20 °C): 126.8 (d, J = 211 Hz), 113.5 (d, J = 209 Hz).
IR (ATR, cm^{-1}): 1958 ($\nu_{C=O}$).

trans/*cis*-[Fe(PNP^{Clpym}-iPr)(CO)$_2$Cl]SbF$_6$ [66] (2f/2g)

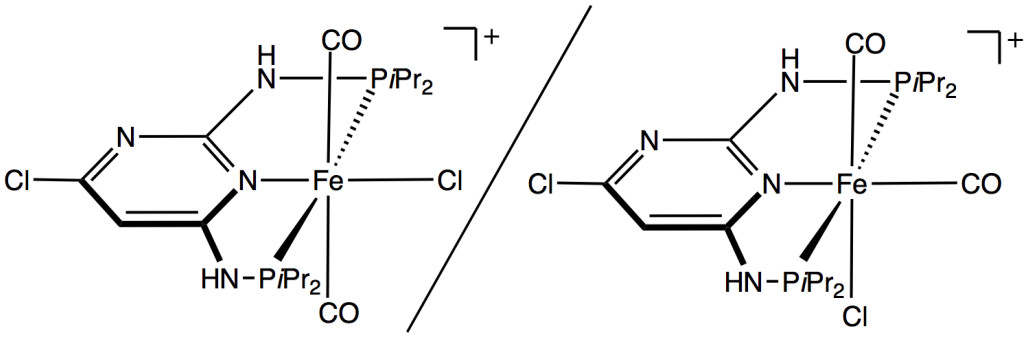

This complex was prepared analogously to **1f** with **2d** (1.4 g, 2.63 mmol) and $AgSbF_6$ (958 mg, 2.63 mmol) as starting materials. A 42:58 mixture of the *cis*/*trans* isomers was obtained.

Yield: 1.74 g (87%) red solid; $C_{18}H_{31}Cl_2F_6FeN_4O_2P_2Sb$ (MW: 759.91); 28.45% C, 4.11% H, 9.33% Cl, 15.00% F, 7.35% Fe, 7.37% N, 4.21%O, 8.15% P, 16.02% Sb.

***trans*-[Fe(PNP^{Clpym}-iPr)(CO)$_2$Cl]SbF$_6$**
^{1}H NMR (δ, acetone-d_6, 20 °C): 8.76 (bs, 2H, NH), 6.37 (bs, 1H, pym^5), 3.17 (bs, 4H, CH(CH$_3$)$_2$), 1.39-1.08 (m, 24H, CH(CH_3)$_2$).

^{31}P{^{1}H} NMR (δ, acetone-d_6, 20 °C): 127.6 (d, J = 84 Hz), 113.0 (d, J = 84 Hz).
IR (ATR, cm^{-1}): 2021 ($\nu_{C=O}$).

***cis*-[Fe(PNP^{Clpym}-iPr)(CO)$_2$Cl]SbF$_6$**

^{1}H NMR (δ, acetone-d_6, 20 °C): 9.09 (bs, 2H, NH), 6.67 (bs, 1H, pym^{5}), 3.43 (bs, 4H, CH(CH$_3$)$_2$), 1.69-1.51 (m, 24H, CH(CH_3)$_2$).
^{31}P{^{1}H} NMR (δ, acetone-d_6, 20 °C): 146.5 (d, J = 149 Hz), 129.9 (d, J = 149 Hz).
IR (ATR, cm^{-1}): 2057 ($\nu_{C=O}$), 2021 ($\nu_{C=O}$).

Fe(PNP^{OEtpym}-iPr)Cl$_2$ [64] (3d)

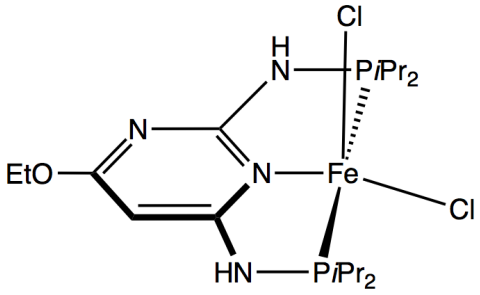

This complex was prepared analogously to **1c** with FeCl$_2$ (230 mg, 1.81 mmol) and **3c** (700 mg, 1.81 mmol) as starting materials.

Yield: 920 mg (99%) yellow solid; $C_{18}H_{36}Cl_2FeN_4OP_2$ (MW: 513.20); 42.13% C, 7.07% H, 13.82% Cl, 10.88% Fe, 10.92% N, 3.12% O, 12.07% P.
^{1}H NMR (δ, acetone-d_6, 20 °C): 146.54 (s, 2H, CH(CH$_3$)$_2$), 144.72 (s, 2H, CH(CH$_3$)$_2$), 75.92 (s, 1H, NH), 68.80 (s, 1H, NH), 32.01 (s, 1H, pym^{5}), 13.11 (s, 6H, CH(CH_3)$_2$), 12.95 (s, 6H, CH(CH_3)$_2$), 7.12 (s, 12H, CH(CH_3)$_2$), 5.89 (s, 2H, OCH_2CH$_3$), -0.22 (s, 3H, OCH$_2$CH_3).

***trans*-[Fe(PNP^{OEtpym}-iPr)(CO)Cl$_2$] [64] (3e)**

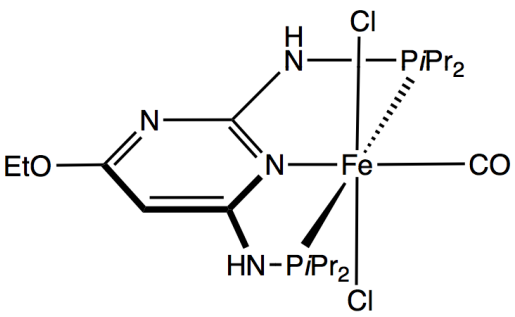

This complex was prepared analogously to **1d** with **3d** (920 mg, 1.79 mmol) as starting material.

Yield: 961 mg (99%) violet solid; $C_{19}H_{36}Cl_2FeN_4O_2P_2$ (MW: 541.21); 42.17% C, 6.70% H, 13.10% Cl, 10.32% Fe, 10.35% N, 5.91%O, 11.45% P.
^{1}H NMR (δ, DMSO-d_6, 20 °C): 9.10 (d, J = 4.8 Hz, 1H, NH), 8.94 (d, J = 5.1 Hz, 1H, NH), 5.94 (s, 1H, pym^5), 4.36 (q, J = 6.9 Hz, 2H, OCH_2CH$_3$), 2.85-2.71 (m, 4H, CH(CH$_3$)$_2$), 1.49-1.23 (m, 27 H, OC$_2$CH_3 and CH(CH_3)$_2$).
^{31}P{^{1}H} NMR (δ, DMSO-d_6, 20 °C): 138.8 (d, J = 177 Hz), 126.2 (d, J = 177 Hz).
IR (ATR, cm^{-1}): 1958 ($\nu_{C=O}$).

cis-[Fe(PNP^{OEtpym}-iPr)(CO)Cl$_2$] [64] (3f)

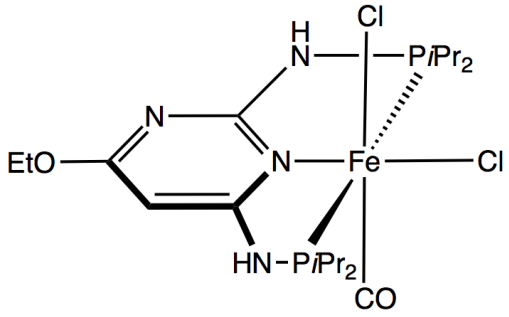

This complex was prepared analogously to **1e** with **3d** (500 mg, 0.97 mmol) as starting material.

Yield: 527 mg (100%) red solid; $C_{19}H_{36}Cl_2FeN_4O_2P_2$ (MW: 541.21); 42.17% C, 6.70% H, 13.10% Cl, 10.32% Fe, 10.35% N, 5.91%O, 11.45% P.
^{1}H NMR (δ, DMSO-d_6, 20 °C): 8.72 (bs, 2H, NH), 5.46 (s, 1H, pym^5), 4.02 (s, 2H, OCH_2CH$_3$), 2.45 (s, 4H, CH(CH$_3$)$_2$), 1.33-1.01 (m, 27H, CH(CH_3)$_2$ and OCH$_2$CH_3).
^{31}P{^{1}H} NMR (δ, DMSO-d_6, 20 °C): 123.9 (d, J = 234 Hz), 112.4 (d, J = 234 Hz).
IR (ATR, cm^{-1}): 1955 ($\nu_{C=O}$).

trans-[Fe(PNP^{OEtpym}-iPr)(CO)$_2$Cl]SbF$_6$ [66] (3g)

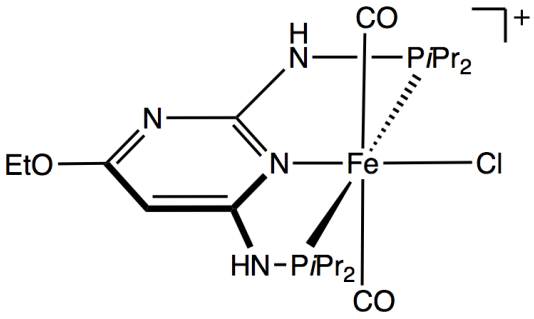

This complex was prepared analogously to **1f** with **3e** (690 mg, 1.27 mmol) and $AgSbF_6$ (438 mg, 1.27 mmol) as starting materials.

Yield: 810 g (83%) red solid; $C_{20}H_{36}ClF_6FeN_4O_3P_2Sb$ (MW: 769.52); 31.22% C, 4.72% H, 4.61% Cl, 14.80% F, 7.26% Fe, 7.28% N, 6.24%O, 8.05% P, 15.82% Sb.

^{1}H NMR (δ, acetone-d_6, 20 °C): 8.58 (s, 1H, NH), 8.41 (s, 1H, NH), 5.68 (s, 1H, pym^5), 4.21 (q, J = 6.7 Hz, 2H, OCH_2CH$_3$), 3.43 (m, 4H, CH(CH$_3$)$_2$), 1.72-1.10 (m, 27H, OCH$_2$CH_3 and OCH$_2$CH_3).
^{13}C{^{1}H} NMR (δ, acetone-d_6, 20 °C): 208.4 (t, J = 23.3 Hz, CO), 170.0 (pym^4), 167.2 (pym^6), 165.9 (d, J = 1.7 Hz, pym^2), 81.7 (d, J = 10.3 Hz, pym^5), 63.1 (OCH$_2$CH$_3$), 30.2 (d, J = 21.8 Hz, CH(CH$_3$)$_2$), 29.7 (d, J = 23.0 Hz, CH(CH$_3$)$_2$), 15.5 (d, J = 5.2 Hz, CH(CH$_3$)$_2$), 10.9 (OCH$_2$$CH_3$).
^{31}P{^{1}H} NMR (δ, acetone-d_6, 20 °C): 124.9 (d, J = 83 Hz), 112.4 (d, J = 83 Hz).
IR (ATR, cm^{-1}): 2014 ($\nu_{C=O}$).

Fe(PNP^{OIsopym}-iPr)Cl$_2$ (4d)

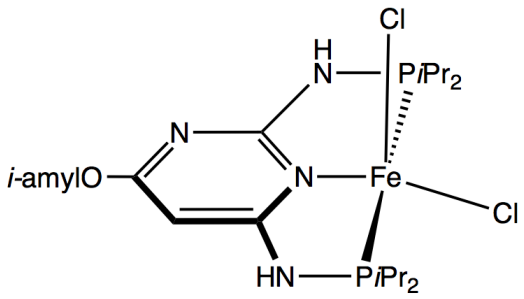

This complex was prepared analogously to **1c** with $FeCl_2$ (169 mg, 1.33 mmol) and **4c** (571 mg, 1.33 mmol) as starting materials.

Yield: 726 mg (98%) white solid; $C_{21}H_{42}Cl_2FeN_4OP_2$ (MW: 555.28); 45.42% C, 7.62% H, 12.77% Cl, 10.06% Fe, 10.09% N, 2.88% O, 11.16% P.

^{1}H NMR (δ, acetone-d_6, 20 °C): 145.21 (s, 2H, CH(CH$_3$)$_2$), 142.81 (s, 2H, CH(CH$_3$)$_2$), 77.61 (s, 1H, NH), 70.09 (s, 1H, NH), 31.56 (s, 1H, pym^5), 13.08 (s, 12H, CH(CH_3)$_2$), 7.37 (s, 12H, CH(CH_3)$_2$), 6.07 (s, 2H, OCH_2CH$_2$CH(CH$_3$)$_2$), 2.05-0.13 (m, 9H, OCH$_2$CH_2CH(CH_3)$_2$).

***trans*-[Fe(PNP^{OIsopym}-iPr)(CO)Cl$_2$] (4e)**

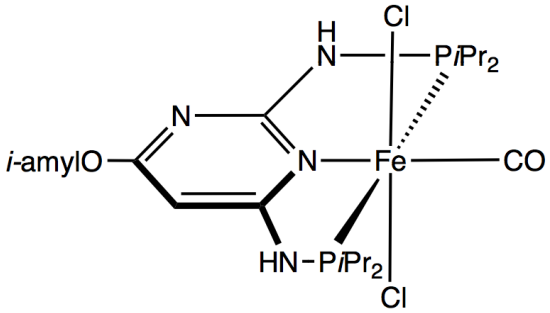

This complex was prepared analogously to **1d** with **4d** (726 mg, 1.31 mmol) as starting material.

Yield: 755 mg (99%) violet solid; $C_{22}H_{42}Cl_2FeN_4O_2P_2$ (MW: 583.29); 45.30% C, 7.26% H, 12.16% Cl, 9.57% Fe, 9.61% N, 5.49%O, 10.62% P.

^{1}H NMR (δ, DMSO-d_6, 20 °C): 9.06 (d, J = 5.3 Hz, 1H, NH), 8.95 (d, J = 4.7 Hz, 1H, NH), 5.96 (s, 1H, pym^5), 4.30 (t, J = 6.4 Hz, 2H, OCH_2CH$_2$CH(CH$_3$)$_2$), 2.87-2.68 (m, 4H, CH(CH$_3$)$_2$), 1.79-1.67 (m, 1 H, OCH$_2$CH$_2$CH(CH$_3$)$_2$), 1.58 (q, J = 6.5 Hz, 2H, OCH$_2$CH_2CH-(CH$_3$)$_2$), 1.47-1.22 (m, 24H, CH(CH_3)$_2$), 0.90 (d, J = 6.4 Hz, 6H, OCH$_2$CH$_2$CH(CH_3)$_2$).

^{13}C{^{1}H} NMR (δ, DMSO-d_6, 20 °C): 224.3 (t, J = 21.8, CO), 170.9 (pym^4), 169.4 (dd, J = 6.0 Hz, J = 13.5 Hz, pym^6), 167.3 (dd, J = 5.5 Hz, J = 19.9 Hz, pym^2), 80.5 (d, J = 7.7 Hz, pym^5), 65.4 (OCH$_2$CH$_2$CH(CH$_3$)$_2$), 37.8 (OCH$_2$$CH_2$CH(CH$_3$)$_2$), 25.6 ($C$H(CH$_3$)$_2$), 25.2 ($C$H(CH$_3$)$_2$), 23.0 (OCH$_2CH_2$$C$H(CH$_3$)$_2$), 19.4 (d, J = 4.0 Hz, CH(CH$_3$)$_2$), 19.3 (d, J = 3.9 Hz, CH(CH$_3$)$_2$), 18.2 (OCH$_2$CH$_2$CH(CH$_3$)$_2$).

^{31}P{^{1}H} NMR (δ, DMSO-d_6, 20 °C): 140.0 (d, J = 179), 127.0 (d, J = 179).

IR (ATR, cm^{-1}): 1967 ($\nu_{C=O}$).

cis-[Fe(PNP^{OIsopym}-iPr)(CO)Cl_2] (4f)

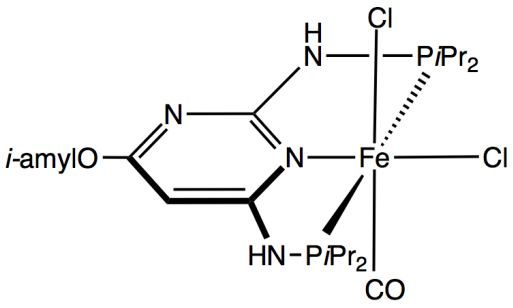

This complex was prepared analogously to **1e** with **4d** (500 mg, 0.97 mmol) as starting material.

Yield: 525 mg (100%) red solid; $C_{22}H_{42}Cl_2FeN_4O_2P_2$ (MW: 583.29); 45.30% C, 7.26% H, 12.16% Cl, 9.57% Fe, 9.61% N, 5.49%O, 10.62% P.
$^{31}P\{^1H\}$ NMR (δ, DMSO-d_6, 20 °C): 123.7 (d, J = 206 Hz), 112 (d, J = 206 Hz).
IR (ATR, cm^{-1}): 1956 ($\nu_{C=O}$).

trans/*cis*-[Fe(PNP^{OIsopym}-iPr)$(CO)_2$Cl]SbF_6 (4g/4h)

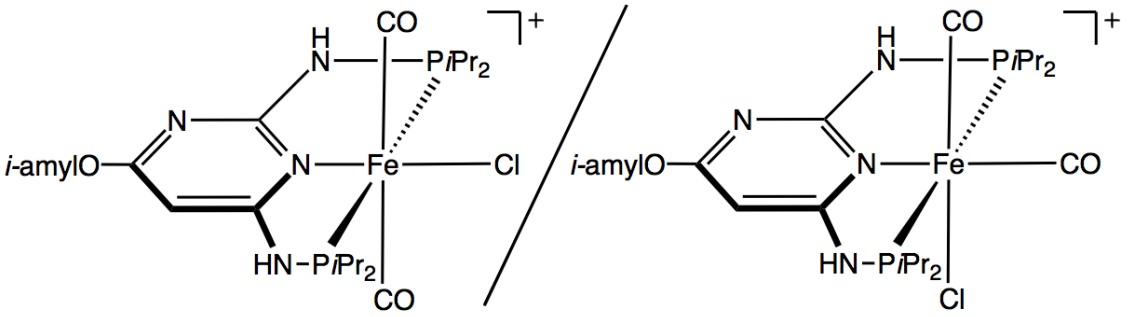

This complex was prepared analogously to **1f** with **4e** (1.5 g, 2.57 mmol) and $AgSbF_6$ (884 mg, 2.57 mmol) as starting materials. A 29:71 mixture of the *cis*/*trans* isomers was obtained.

Yield: 1.88 g (90%) red solid; $C_{23}H_{42}ClF_6FeN_4O_3P_2Sb$ (MW: 811.60); 34.04% C, 5.22% H, 4.37% Cl, 14.05% F, 6.88% Fe, 6.90% N, 5.91%O, 7.63% P, 15.00% Sb.

trans-[Fe(PNP^{OIsopym}-iPr)$(CO)_2$Cl]SbF_6

^1H NMR (δ, acetone-d_6, 20 °C): 8.49 (s, 1H, NH), 8.31 (s, 1H, NH), 5.68 (s, 1H, pym[5]), 4.18 (s, 2H, OC$H_2$$CH_2$$CH(CH_3)_2$), 3.59-3.00 (m, 4H, C$H(CH_3)_2$), 1.61-0.89 (m, 33H,

$CH(CH_3)_2$ and $OCH_2CH_2CH(CH_3)_2$).

$^{13}C\{^1H\}$ NMR (δ, acetone-d_6, 20 °C): 210.3 (t, J = 19.1 Hz, CO), 171.5 (pym^4), 166.7 (d, J = 10.4 Hz, pym^6), 165.2 (d, J = 13.4 Hz, pym^2), 83.3 (pym^5), 66.7 ($OCH_2CH_2CH(CH_3)_2$), 37.7 ($OCH_2CH_2CH(CH_3)_2$), 27.8 ($CH(CH_3)_2$), 24.9 ($OCH_2CH_2CH(CH_3)_2$), 22.5 ($OCH_2CH_2CH(CH_3)_2$), 18.9 ($CH(CH_3)_2$), 18.7 ($CH(CH_3)_2$), 18.5 ($CH(CH_3)_2$), 18.3 ($CH(CH_3)_2$).

$^{31}P\{^1H\}$ NMR (δ, acetone-d_6, 20 °C): 124.9 (d, J = 83 Hz), 112.5 (d, J = 83 Hz).

IR (ATR, cm^{-1}): 2012 ($\nu_{C=O}$).

***cis*-[Fe(PNP^{OIsopym}-iPr)(CO)$_2$Cl]SbF$_6$**

^1H NMR (δ, acetone-d_6, 20 °C): 8.79 (s, 1H, NH), 8.57 (s, 1H, NH), 5.96 (s, 1H, pym^5), 4.31 (s, 2H, $OCH_2CH_2CH(CH_3)_2$), 3.59-3.00 (m, 4H, $CH(CH_3)_2$), 1.61-0.89 (m, 33H, $CH(CH_3)_2$ and $OCH_2CH_2CH(CH_3)_2$).

$^{13}C\{^1H\}$ NMR (δ, acetone-d_6, 20 °C): 211.8 (t, J = 24.4 Hz, CO), 171.7 (pym^4), 167.7 (d, J = 11.3 Hz, pym^6), 165.9 (d, J = 10.5 Hz, pym^2), 83.3 (pym^5), 66.7 ($OCH_2CH_2CH(CH_3)_2$), 37.7 ($OCH_2CH_2CH(CH_3)_2$), 28.3 ($CH(CH_3)_2$), 24.9 ($OCH_2CH_2CH(CH_3)_2$), 22.6 ($OCH_2CH_2CH(CH_3)_2$), 19.5 ($CH(CH_3)_2$), 19.2 ($CH(CH_3)_2$), 18.1 ($CH(CH_3)_2$), 17.9 ($CH(CH_3)_2$).

$^{31}P\{^1H\}$ NMR (δ, acetone-d_6, 20 °C): 143.1 (d, J = 149 Hz), 128.6 (d, J = 149 Hz).

IR (ATR, cm^{-1}): 2045 ($\nu_{C=O}$), 1995 ($\nu_{C=O}$).

12.2 PNP-Ph Complexes

[Fe(PNP-Ph)$_2$Cl]BF$_4$ (1h)

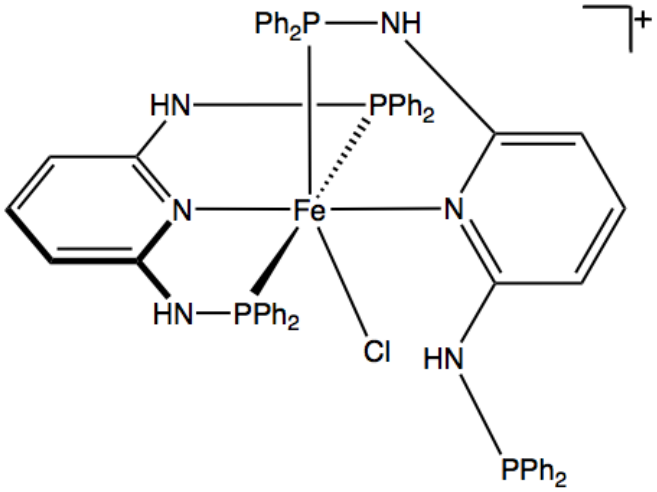

To a solution of PNP-Ph **1a** (1.4 g, 2.92 mmol) and $NaBF_4$ (641 mg, 5.84 mmol) in THF $FeCl_2$ (185 mg, 1.46 mmol) was added. The reaction mixture was stirred for 3h. After the solids were filtered off the solvent was removed under reduced pressure. The remaining green solid was washed thrice with Et_2O (10mL) and dried under vacuum.

Yield: 1.56 g (94%) green solid; $C_{58}H_{50}BClF_4FeN_6P_4$ (MW: 1133.05); 61.48% C, 4.45% H, 0.95% B, 3.13% Cl, 6.71% F, 4.39% Fe, 7.42% N, 10.93% P.
^{1}H NMR (δ, THF-d_8, 20 °C): 8.97-8.82 (m, 4H, N*H*), 7.80-6.75 (m, 46H, Ph and py^{3,4,5}).
^{13}C{^{1}H} NMR (δ, THF-d_8, 20 °C): 131.3-125.3 (m, Ph, py).
^{31}P{^{1}H} NMR (δ, THF-d_8, 20 °C): 107.3 (d,J = 50.2), 105.8 (d, J = 49.3), 101.9, 43.7.

cis-[Fe(PNP-Ph)(CO)Cl_2] (1i)

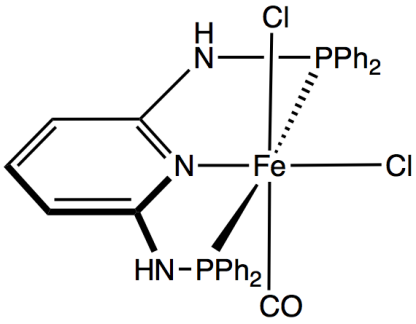

CO was bubbled into a solution of PNP-Ph (697 mg, 1.46 mmol) in acetone and $FeCl_2$ (185 mg, 1.46 mmol) was added. CO was applied for further 10 minutes. The solvent was then removed under reduced pressure and the remaining red solid washed thrice with Et_2O (10 mL) and dried under vacuum.

Yield: 821 mg (89%) red solid; $C_{30}H_{25}Cl_2FeN_3OP_2$ (MW: 632.24); 56.99% C, 3.99% H, 11.22% Cl, 8.83% Fe, 6.65% N, 2.53%O, 9.80% P.
^{1}H NMR (δ, DMSO-d_6, 20 °C): 9.81 (bs, 2H, N*H*), 8.16-7.26 (m, 21H, Ph and py^4), 6.37 (bs, 2H, py^{3,5}).
^{13}C{^{1}H} NMR (δ, DMSO-d_6, 20 °C): 162.3 (t, J = 18.4 Hz, *C*O), 132.8 (py^{2,6}), 130.7 (py^4), 130.2 (Ph^1), 129.4 (Ph^{2,6}), 128.9 (Ph^4), 128.1 (Ph^{3,5}), 99.5 (m, py^{3,5}).
^{31}P{^{1}H} NMR (δ, DMSO-d_6, 20 °C): 100.2.
IR (ATR, cm^{-1}): 1958 ($\nu_{C=O}$).

$[Fe(PNP^{Clpym}\text{-}Ph)_2Cl]BF_4$ (2h)

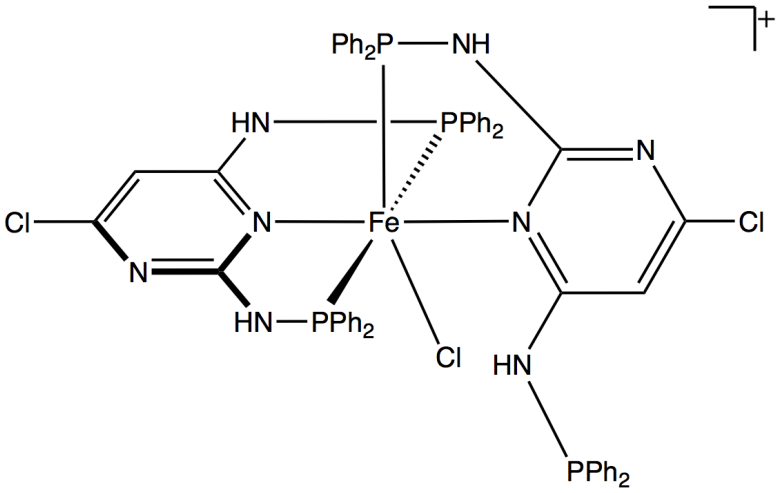

This complex was prepared analogously to **1h** with **2a** (1.5 g, 2.92 mmol), $FeCl_2$ (185 mg, 1.46 mmol) and $NaBF_4$ (642 mg, 5.85 mmol) as starting materials.

Yield: 1.68 g (95%) green solid; $C_{56}H_{46}BCl_3F_4FeN_8P_4$ (MW: 1203.92); 57.06% C, 4.55% H, 0.86% B, 8.42% Cl, 6.02% F, 4.42% Fe, 8.87% N, 9.81% P.

^{1}H NMR (δ, acetone-d_6, 20 °C): 10.02 (d, J = 4.9 Hz, 1H, NH), 9.96 (s, 1H, NH), 9.87 (s, 1H, NH), 9.77 (s, 1H, NH), 7.88-6.96 (m, 41H, Ph and pym[5])
^{13}C{^{1}H} NMR (δ, acetone-d_6, 20 °C): 131.4-125.8 (m, Ph and pym)
^{31}P{^{1}H} NMR (δ, acetone-d_6, 20 °C): 112.5 (dd, J = 46 Hz, J = 153 Hz), 106.4 (t, J = 48 Hz), 98.9 (dd, J = 49 Hz, J = 152 Hz), 35.9.

cis-$[Fe(PNP^{Clpym}\text{-}Ph)(CO)Cl_2]$ (2i)

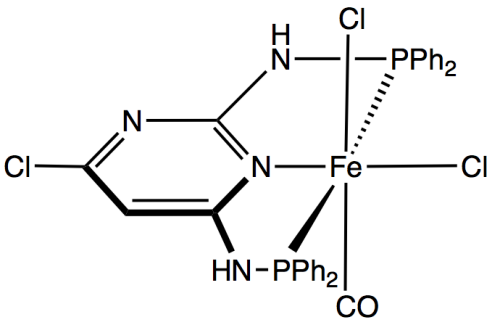

This complex was prepared analogously to **1i** with **2a** (1.5 g, 2.92 mmol) and $FeCl_2$ (371 mg, 2.92 mmol) as starting materials.

Yield: 1.76 g (90%) red solid; $C_{29}H_{23}Cl_3FeN_4OP_2$ (MW: 667.67); 52.17% C, 3.47% H, 15.93% Cl, 8.36% Fe, 8.39% N, 2.4%O, 9.28% P.

^{1}H NMR (δ, DMSO-d_6, 20 °C): 11.18 (s, 1H, NH), 10.78 (s, 1H, NH), 8.06-6.57 (m, 23H, Ph and pym[5])

^{31}P{^{1}H} NMR (δ, DMSO-d_6, 20 °C): 106.8 (d, J = 249 Hz), 94.5 (d, J = 249 Hz).

Part IV

Appendix

References

[1] C. P. Casey and H. Guan, Journal of the American Chemical Society **129**, 5816 (2007).

[2] C. Sui-Seng, F. Freutel, A. Lough, and R. Morris, Angewandte Chemie **120**, 954 (2008).

[3] R. Langer, G. Leitus, Y. Ben-David, and D. Milstein, Angewandte Chemie International Edition **50**, 2120 (2011).

[4] J. W. Peters, W. N. Lanzilotta, B. J. Lemon, and L. C. Seefeldt, Science **282**, 1853 (1998).

[5] D. Benito-Garagorri and K. Kirchner, Accounts of Chemical Research **41**, 201 (2008).

[6] M. D. Fryzuk, T. Haddad, and D. J. Berg, Coordination Chemistry Reviews **99**, 137 (1990).

[7] R. G. Nuzzo, S. L. Haynie, M. E. Wilson, and G. M. Whitesides, The Journal of Organic Chemistry **46**, 2861 (1981).

[8] L. Sacconi and R. Morassi, J. Chem. Soc. A , 2997 (1968).

[9] L.-C. Liang, J.-M. Lin, and C.-H. Hung, Organometallics **22**, 3007 (2003).

[10] A. Castonguay, C. Sui-Seng, D. Zargarian, and A. L. Beauchamp, Organometallics **25**, 602 (2006).

[11] A. A. Danopoulos, A. A. D. Tulloch, S. Winston, G. Eastham, and M. B. Hursthouse, Dalton Trans. , 1009 (2003).

[12] K. Peveling et al., Organometallics **23**, 1501 (2004).

[13] Q. Yao and M. Sheets, The Journal of Organic Chemistry **71**, 5384 (2006).

[14] H.-J. v. Manen et al., European Journal of Inorganic Chemistry **2000**, 2533 (2000).

[15] W. V. Dahlhoff and S. M. Nelson, J. Chem. Soc. A , 2184 (1971).

[16] C. J. Moulton and B. L. Shaw, J. Chem. Soc., Dalton Trans. , 1020 (1976).

[17] G. van Koten, K. Timmer, J. G. Noltes, and A. L. Spek, J. Chem. Soc., Chem. Commun. , 250 (1978).

[18] C. S. Creaser and W. C. Kaska, Inorganica Chimica Acta **30**, L325 (1978).

[19] H. Rimml and L. M. Venanzi, Journal of Organometallic Chemistry **259**, C6 (1983).

[20] M. Albrecht and G. van Koten, Angewandte Chemie International Edition **40**, 3750 (2001).

[21] J. T. Singleton, Tetrahedron **59**, 1837 (2003).

[22] W. Schirmer, U. Flörke, and H. Haupt, Zeitschrift für anorganische und allgemeine Chemie **545**, 83 (1987).

[23] D. Benito-Garagorri et al., Organometallics **25**, 1900 (2006).

[24] D. Benito-Garagorri, V. Bocokic, K. Mereiter, and K. Kirchner, Organometallics **25**, 3817 (2006).

[25] D. Benito-Garagorri, I. Lagoja, L. F. Veiros, and K. A. Kirchner, Dalton Trans. **40**, 4778 (2011).

[26] N. Alberding et al., Biophysical Journal **24**, 319 (1978).

[27] B. H. McMahon, B. P. Stojkovic, P. J. Hay, R. L. Martin, and A. E. Garcia, The Journal of Chemical Physics **113**, 6831 (2000).

[28] D. W. Thompson et al., Inorganic Chemistry **42**, 5211 (2003).

[29] J. N. Harvey, Journal of the American Chemical Society **122**, 12401 (2000).

[30] Y. Nicolet, C. Piras, P. Legrand, C. E. Hatchikian, and J. C. Fontecilla-Camps, Structure **7**, 13 (1999).

[31] M. Y. Darensbourg, E. J. Lyon, and J. J. Smee, Coordination Chemistry Reviews **206–207**, 533 (2000).

[32] J. Huhmann-Vincent, B. L. Scott, and G. J. Kubas, Inorganica Chimica Acta **294**, 240 (1999).

[33] S. Niu, L. M. Thomson, and M. B. Hall, Journal of the American Chemical Society **121**, 4000 (1999).

[34] F. A. Armstrong, Current Opinion in Chemical Biology **8**, 133 (2004).

[35] A. Volbeda and J. C. Fontecilla-Camps, Dalton Trans. , 4030 (2003).

[36] S. Reissmann et al., Science **299**, 1067 (2003).

[37] R. K. Thauer, A. R. Klein, and G. C. Hartmann, Chemical Reviews **96**, 3031 (1996).

[38] R. Cammack, Nature **397**, 214 (1999).

[39] J. N. Harvey, R. Poli, and K. M. Smith, Coordination Chemistry Reviews **238–239**, 347 (2003), ¡ce:title¿Theoretical and Computational Chemistry¡/ce:title¿.

[40] J. N. Harvey, Phys. Chem. Chem. Phys. **9**, 331 (2007).

[41] P. Dani, T. Karlen, R. A. Gossage, S. Gladiali, and G. van Koten, Angewandte Chemie International Edition **39**, 743 (2000).

[42] J. Yao, W. T. Wong, and G. Jia, Journal of Organometallic Chemistry **598**, 228 (2000).

[43] M. Gupta, C. Hagen, W. C. Kaska, R. E. Cramer, and C. M. Jensen, Journal of the American Chemical Society **119**, 840 (1997).

[44] G. Bauer and K. A. Kirchner, Angewandte Chemie International Edition **50**, 5798 (2011).

[45] H.-U. Blaser et al., Advanced Synthesis & Catalysis **345**, 103 (2003).

[46] F. Naud, F. Spindler, C. J. Rueggeberg, A. T. Schmidt, and H.-U. Blaser, Organic Process Research & Development **11**, 519 (2007).

[47] R. H. Crabtree, New J. Chem. **35**, 18 (2011).

[48] H. Grützmacher, Angewandte Chemie International Edition **47**, 1814 (2008).

[49] J. I. van der Vlugt and J. N. H. Reek, Angewandte Chemie International Edition **48**, 8832 (2009).

[50] R. M. Bullock, Chemistry – A European Journal **10**, 2366 (2004).

[51] J. A. Wright, P. J. Turrell, and C. J. Pickett, Organometallics **29**, 6146 (2010).

[52] C. Tard and C. J. Pickett, Chemical Reviews **109**, 2245 (2009), PMID: 19438209.

[53] R. H. Morris, Chem. Soc. Rev. **38**, 2282 (2009).

[54] S. Enthaler, K. Junge, and M. Beller, Angewandte Chemie International Edition **47**, 3317 (2008).

[55] S. Gaillard and J.-L. Renaud, ChemSusChem **1**, 505 (2008).

[56] C. Bolm, J. Legros, J. Le Paih, and L. Zani, Chemical Reviews **104**, 6217 (2004), PMID: 15584700.

[57] S. Enthaler, B. Hagemann, G. Erre, K. Junge, and M. Beller, Chemistry – An Asian Journal **1**, 598 (2006).

[58] H.-J. Knölker, E. Baum, H. Goesmann, and R. Klauss, Angewandte Chemie International Edition **38**, 2064 (1999).

[59] C. Sui-Seng et al., Inorganic Chemistry **48**, 735 (2009).

[60] M.-Y. Jang, S. D. Jonghe, K. Segers, J. Anne, and P. Herdewijn, Bioorg. Med. Chem. **19**, 702 (2011).

[61] C. P. Casey and H. Guan, Journal of the American Chemical Society **131**, 2499 (2009).

[62] R. Langer, G. Leitus, Y. Ben-David, and D. Milstein, Angewandte Chemie **123**, 2168 (2011).

[63] D. Benito-Garagorri, J. Wiedermann, M. Pollak, K. Mereiter, and K. Kirchner, Organometallics **26**, 217 (2007).

[64] D. Benito-Garagorri et al., Organometallics **28**, 6902 (2009).

[65] D. Benito-Garagorri, M. Puchberger, K. Mereiter, and K. Kirchner, Angewandte Chemie International Edition **47**, 9142 (2008).

[66] D. Benito-Garagorri et al., Organometallics **29**, 4932 (2010).

[67] W. L. F. Armarego and C. L. L. Chai, *Purification of Laboratory Chemicals*, Elsevier, 2009.